Volume 40, January 2014 ISSN 0883-2927

ELSEVIER

Applied Geochemistry

JOURNAL OF THE INTERNATIONAL ASSOCIATION OF GEOCHEMISTRY

Continued on outside back cover

Applied Geochemistry 40 (2014) 164–179

Contents lists available at ScienceDirect

Applied Geochemistry

journal homepage: www.elsevier.com/locate/apgeochem

$^{234}U/^{238}U$ and $\delta^{87}Sr$ in peat as tracers of paleosalinity in the Sacramento-San Joaquin Delta of California, USA

J.Z. Drexler [a,*], J.B. Paces [b], C.N. Alpers [a], L. Windham-Myers [c], L.A. Neymark [b], T.D. Bullen [c], H.E. Taylor [d]

[a] U.S. Geological Survey, California Water Science Center, 6000 J Street, Placer Hall, Sacramento, CA 95819, United States
[b] U.S. Geological Survey, Geosciences and Environmental Change Science Center, Box 25046, Denver Federal Center, Mail Stop 963, Denver, CO 80225, United States
[c] U.S. Geological Survey, Building 15, McKelvey Blg., Mail Stop 480, 345 Middlefield Road, Menlo Park, CA 94025, United States
[d] U.S. Geological Survey, 3215 Marine Street, Suite E-127, Boulder, CO 80303, United States

ARTICLE INFO

Article history:
Received 16 May 2013
Accepted 25 October 2013
Available online 1 November 2013
Editorial handling by M. Kersten

ABSTRACT

The purpose of this study was to determine the history of paleosalinity over the past 6000+ years in the Sacramento-San Joaquin Delta (the Delta), which is the innermost part of the San Francisco Estuary. We used a combination of Sr and U concentrations, $\delta^{87}Sr$ values, and $^{234}U/^{238}U$ activity ratios (AR) in peat as proxies for tracking paleosalinity. Peat cores were collected in marshes on Browns Island, Franks Wetland, and Bacon Channel Island in the Delta. Cores were dated using ^{137}Cs, the onset of Pb and Hg contamination from hydraulic gold mining, and ^{14}C. A proof of concept study showed that the dominant emergent macrophyte and major component of peat in the Delta, *Schoenoplectus* spp., incorporates Sr and U and that the isotopic composition of these elements tracks the ambient water salinity across the Estuary. Concentrations and isotopic compositions of Sr and U in the three main water sources contributing to the Delta (seawater, Sacramento River water, and San Joaquin River water) were used to construct a three-end-member mixing model. Delta paleosalinity was determined by examining variations in the distribution of peat samples through time within the area delineated by the mixing model.

The Delta has long been considered a tidal freshwater marsh region, but only peat samples from Franks Wetland and Bacon Channel Island have shown a consistently fresh signal (<0.5 ppt) through time. Therefore, the eastern Delta, which occurs upstream from Bacon Channel Island along the San Joaquin River and its tributaries, has also been fresh for this time period. Over the past 6000+ years, the salinity regime at the western boundary of the Delta (Browns Island) has alternated between fresh and oligohaline (0.5–5 ppt).

Published by Elsevier Ltd.

1. Introduction

Peat soils and wetland sediments are well known as archives of environmental change and contamination (e.g., Shotyk, 1996; Byrne et al., 2001; Charman, 2002). Within these archives there exist numerous proxies that can be used to address questions regarding climate change, hydrological processes, environmental contamination, and paleosalinity (Ingram et al., 1996; Charman, 2002; Van der Putten et al., 2012). With regard to paleosalinity, several proxies such as pollen, stratigraphic seed data, $\delta^{13}C$ in diatoms and foraminifera, and B, Br, Na, S, Ge, and U concentrations in peat have been used to characterize salinity regimes through the millennia (Goman and Wells, 2000; Malamud-Roam and Ingram, 2004; Di Rita et al., 2011). In addition, $\delta^{87}Sr$ in fossil bivalves found within saline and brackish estuarine sediments has been shown to be a particularly effective tracer (Ingram and Sloan, 1992; Ingram and DePaolo, 1993; Ingram et al., 1996). However, fossil bivalves are not common or well distributed in tidal freshwater marshes, which are found in the inner reaches of estuaries. Therefore, a different proxy is needed to determine paleosalinity in tidal freshwater marshes.

The natural chemistry of peat may, in and of itself, be a useful proxy for paleosalinity, if certain conditions are met. First of all, the tracer being considered must differ in concentration between freshwater and seawater. Next, the tracer needs to be conservative in nature such that, once sequestered, there is little tendency for subsequent mobility in peat, or be present in sufficient quantity that exchange with ambient water is negligible. Ideally, the tracer should be immune from modification due to changes in state, evaporative concentration, or chemical precipitation under ambient conditions. Finally, the tracer must chiefly reside in the organic component of the peat, which is derived from the plants that grew in a site under a particular salinity regime (López-Buendia et al., 1999). If the provenance of an element in peat is mostly from sediment washed in from the watershed (lithogenic sources), the element cannot trace salinity conditions at the time the plants were growing. Previous research has shown that certain highly insoluble

* Corresponding author. Tel.: +1 916 278 3057; fax: +1 916 278 3071.
E-mail address: jdrexler@usgs.gov (J.Z. Drexler).

0883-2927/$ - see front matter Published by Elsevier Ltd.
http://dx.doi.org/10.1016/j.apgeochem.2013.10.011

elements, such as titanium, are predominantly found in the lithogenic fraction of peat and remain highly immobile once incorporated into the peat matrix (Shotyk, 1996; López-Buendia et al., 1999; Novak et al., 2011). Such highly insoluble elements have been used to "normalize" the sediment variability in the peat matrix. This allows for clear identification of elements chiefly found in the organic fraction of peat (i.e., those lacking a relationship with Ti), which constitute the potential proxies for paleosalinity.

The purpose of this study was to determine the history of paleosalinity over the past 6000+ years in the Sacramento-San Joaquin Delta (the Delta), which is the innermost part of the San Francisco Estuary. We used a combination of Sr and U concentrations, $\delta^{87}Sr$ values, and $^{234}U/^{238}U$ activity ratios (AR) in peat as proxies for tracking paleosalinity. We chose U and Sr because, similar to Ca, Mg, K, and Na, they are readily soluble across the salinity spectrum and have distinct concentrations in freshwater vs. sea water (Table 1). Furthermore, they each have heavy, radiogenic isotope compositions that may be unique to each water source and can be used concomitantly as hydrologic tracers. The benefit of this approach is that, unlike elemental concentrations, which under near-surface conditions are affected by a variety of processes and chemical reactions that can result in complex geochemical behavior, $^{87}Sr/^{86}Sr$ and $^{234}U/^{238}U$ are largely immune from fractionation caused by near-surface physical, chemical, and biological processes (Faure and Powell, 1972; Hart et al., 2004). Furthermore, Sr is plentiful in ocean water relative to river water and Sr isotopes have previously been used for tracking paleosalinity (Ingram and Sloan, 1992; Ingram and DePaolo, 1993; Ingram et al., 1996). In addition, Sr isotopes have been successfully used as a tracer of provenance in organic materials (Shand et al., 2007; von Carnap-Bornheim et al., 2007). Uranium, which is commonly present at much lower concentrations than Sr, has the extra benefit of being taken up very efficiently and held tightly by the peat matrix under reducing conditions (Szalay, 1964; Idiz et al., 1986; Johnson et al., 1987; Owen et al., 1992; Zielinski et al., 2000; Novak et al., 2011). Therefore, $^{234}U/^{238}U$ isotopic composition of peat can be used as a tracer and independent check on Sr isotope behavior, which may be more susceptible to post-depositional mobility.

We applied our approach using peat cores collected in tidal marshes in the Delta. We first conducted a proof of concept study in the greater San Francisco Estuary to determine whether living plants, which ultimately become the bulk of the peat matrix, track the salinity signal with regard to these tracers. Then we constructed a three-component mixing model for water using a combination of Sr and U concentrations, $\delta^{87}Sr$ values, and $^{234}U/^{238}U$ activity ratios (AR) in the three hydrologic end-members: seawater, Sacramento River water, and San Joaquin River water. The resulting mixing model was compared to the $\delta^{87}Sr$ and $^{234}U/^{238}U$ compositions of marsh peat samples, nearly all of which plotted within the "mixing triangle" delineated by the end members. Delta paleosalinity was determined by examining patterns in the distribution of peat samples through time within the mixing triangle.

Today the Sacramento-San Joaquin Delta is classified as a tidal *freshwater* delta, yet whether this has been the case throughout its ~6700-year history (Drexler et al., 2007) remains largely unknown. Knowledge of the extent and timing of past natural fluctuations would help managers better predict the resilience of the Delta subsequent to the proposed major changes in water conveyance (California Department of Water Resources et al., 2013). Paleosalinity research has been carried out in saline and brackish parts of the San Francisco Estuary but in the upstream reaches, only the western periphery of the Delta (at Browns Island) has been studied (Goman and Wells, 2000; Goman, 2001). The results of this previous research showed that, between 6200 and 3800 calibrated years before present (cal yr BP), paleosalinity at Browns Island was comparable to present values (slightly brackish). A period of fresher salinity was noted between 3800 and 2000 cal yr BP followed by a return to the slightly brackish conditions over the past 2000 years. In order to characterize paleosalinity ranges within the greater Delta system, we studied peat from Browns Island as well as two other sites on a west-east gradient with salinities currently ranging from oligohaline (0.5–5 practical salinity units (psu); where psu is the unitless Practical Salinity Scale on which seawater is ~35) to fresh (<0.5 psu).

2. Study sites

The Sacramento-San Joaquin Delta of California was once a 1400 km^2 region of marshes, channels, and mudflats. Beginning in the mid-1800s, the Delta was largely drained for agriculture (Thompson, 1957), resulting in its current configuration of more than 100 islands and tracts surrounded by 2250 km of man-made levees and 1130 km of waterways (Prokopovich, 1985). Tides in the Delta are semidiurnal and microtidal, with a normal range of approximately one meter (Shlemon and Begg, 1975; Atwater, 1980). The climate in the Delta is characterized as Mediterranean with cool winters and hot, dry summers (Thompson, 1957). Mean annual precipitation is approximately 36 cm, but actual yearly precipitation varies from half to almost four times this amount. Over 80% of precipitation occurs from November through March (Thompson, 1957).

Currently, the water flow in the Delta is highly regulated so the saltwater wedge originating in the San Francisco Bay has little chance to travel much further east than the western boundary of the Delta. However, prior to construction of dams on nearly all major tributaries to the Delta during the 1940s to 1970s, salinity incursions into the Delta could extend as far as the eastern Delta, especially during a dry year (Ingebritsen et al., 2000). Furthermore, in any given year, salinity likely ranged from fresh during the rainy season to slightly brackish or very brackish during the dry season, depending on the amount of annual precipitation. Currently, however, salinity is regulated for the purpose of maintaining water quality as well as managing a parameter called X_2, which is the distance from the mouth of the estuary at the Golden Gate up the axis to where the tidally-averaged bottom salinity is 2 psu (Kimmerer, 2002).

Marsh study sites were chosen along the historic floodplain of the Sacramento River as well as the glacial outwash area along the San Joaquin River (Fig. 1). In addition, sites were selected from high energy environments such as the confluence of the Sacramento and San Joaquin Rivers to more quiescent environments such as distrib-

Table 1
Concentrations (mg l^{-1}) of the major cations Ca, Mg, K, and Na, and minor cations, Sr and U as well as pH in freshwater from the Sacramento and San Joaquin Rivers and seawater. River data were retrieved from the National Water Information System of the U.S. Geological Survey for the period from 1950 to 2010 and represent median concentrations of all measurements, which include all chemical species. Seawater concentrations are from Turekian (1968).

	Ca	Mg	K	Na	Sr	U	pH
San Joaquin River	32	15	3	69	0.389	0.005	7.7
Sacramento River	12	6.1	1.2	9.1	0.091	0.00013	7.7
Seawater	400	1290	392	10800	8.1	0.0033	7.9–8.2

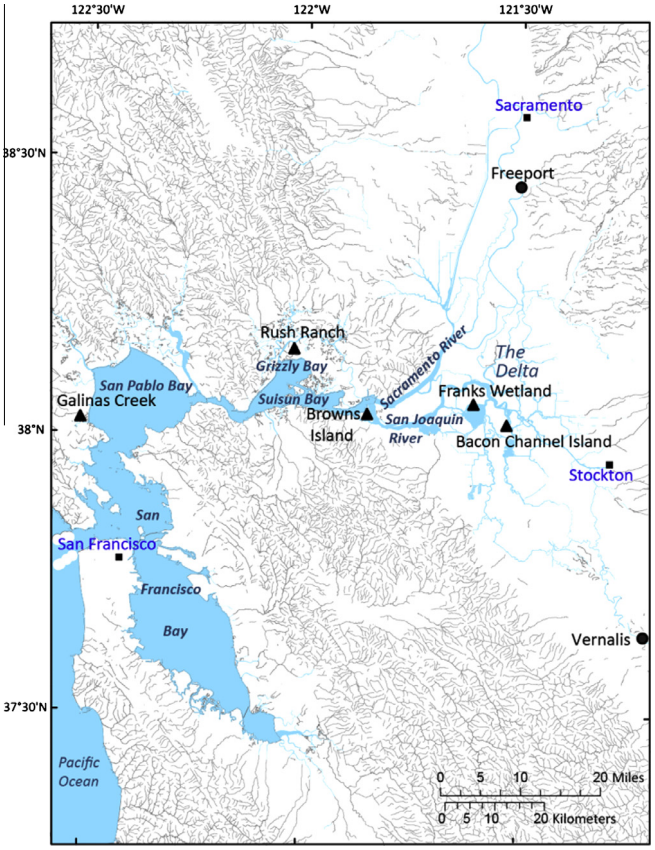

Fig. 1. Map of peat coring and plant collection sites (triangles) and river water collection sites (circles) in the San Francisco Estuary and its watershed, California, USA.

utaries of the San Joaquin River. The three sites, Browns Island (BRI, 268 ha, high energy), Franks Wetland (FW, 28 ha, low energy), and Bacon Channel Island (BACHI, 10 ha, low energy) are relatively undisturbed marshes, which, unlike those in the vast majority of the region, were not converted for agriculture (Drexler et al., 2009a). Vegetation on these natural marsh islands is highly productive and dominated by the emergent macrophytes *Schoenoplectus americanus* (American bulrush), *S. acutus* (hardstem bulrush), *Phragmites australis* (common reed), and *Typha* spp. (cattail) and shrub-scrub wetland species including *Salix lasiolepis* (arroyo willow) and *Cornus sericea* (red-osier dogwood) (Drexler et al., 2009b). Peat deposits at these sites range from seven to over nine meters in depth (Table 2) and contain abundant organic material including decaying plant roots, rhizomes, and stems, some of which are very well preserved (Goman and Wells, 2000; Drexler, 2011). Such preservation of organic material demonstrates that reducing conditions are prevalent in the peat matrix, causing decomposition to proceed along slow, anaerobic pathways (Gambrell and Patrick, 1978). Reducing conditions are typical in tidal marsh soils due to the high water table, which is maintained by the periodicity of the tides (particularly in microtidal regions such as the Delta) as well as the low rates of hydraulic conductivity that keep soils at or near saturation, even during ebb tides (Rabenhorst, 2001).

3. Methods

3.1. Sample collection

In the summer of 2005, peat cores were collected from each marsh site using a modified 5-cm-diameter Livingstone corer (Wright, 1991). At Browns Island, the first core, BRIC4, unlike all the other cores in the study, did not have good recovery near the surface due to a particularly dense root mat. In addition, BRIC4 did not reach the underlying mineral substrate, even though much clay was already present below 700 cm. Therefore, an additional core (BRIC5) that included the entire peat column of 922 cm was collected in March 2007 within 2 m of the BRIC4 site. A soil monolith of approximately 50 × 50 × 50 cm (BRIP) was excavated from the surface to improve recovery over that achieved with the Livingstone corer. Further details about coring can be found in Drexler et al. (2009a).

Real-time kinematic geographic positioning was used to establish the elevations and coordinates of the coring locations. Tidal benchmark LSS 13 (National Oceanic and Atmospheric Administration tidal station 9415064 located near Antioch, CA) with a static surveyed ellipsoid height of −28.75 meters was used to adjust the elevations of the coring sites to local mean sea level. Details concerning peat coring and survey procedures can be found in Drexler et al. (2009b). Overall characteristics of peat at each marsh site as well as marsh surface elevations are included in Table 2.

During November and December 2009, we conducted a proof of concept study to evaluate whether marsh plants reflect the salinity and isotopic signal of the hydrogenic versus lithogenic components within their ambient growth environment. We chose 4 marsh sites in the San Francisco Estuary ranging from brackish to fresh: Galinas Creek in San Pablo Bay, Rush Ranch in Grizzly Bay, and Browns Island and Franks Wetland in the Delta (Fig. 1). We collected entire specimens of *Schoenoplectus californicus* (dominant in Galinas Creek) or *S. acutus* (dominant in the other sites) at three different places within each marsh. These plant species were chosen because (1) they are ubiquitous in most brackish and freshwater tidal marshes in the San Francisco Estuary, and (2) they are emergent macrophytes with large roots and rhizomes, which are the main organic contributors to the peat matrix. Entire plant samples were collected as close as possible to water quality gauges for which long-term salinity data were available. Plant samples were rinsed in the field with ambient water to remove sediment and placed in labeled plastic bags.

Water samples were collected at the U.S. Geological Survey river gauges on the Sacramento River at Freeport and the San Joaquin River at Vernalis (Fig. 1) on March 15 and 16, 2011, respectively. Samples were filtered with a 0.45 μm filter and stored in 500-ml, pre-cleaned high-density polyethylene bottles until analyzed for Sr and U concentrations and isotopic compositions.

3.2. Core processing

In the laboratory, core stratigraphy was documented, cores were split lengthwise and photographed, and one longitudinal half of the core was archived for future use. Bulk density was obtained by sectioning cores into 2-cm-thick blocks, measuring each

Table 2
Elevations and basic descriptions of peat cores from BACHI, BRI, and FW.

Core	Elevation of top of core (m MSL)	Depth of peat column (cm)	Mean bulk density (g cm^{-3}, ±sd)	Mean % organic matter (±sd)
BACHI	0.21	726	0.12 ± 0.05	76 ± 16
BRI	0.51	922	0.31 ± 0.15	40 ± 18
FW	0.27	718[a]	0.14 ± 0.08	72 ± 19

[a] Only the top 608 cm of core were used because deeper peat layers contained inversions in radiocarbon dates, precluding accurate dating.

dimension, obtaining wet weight of the sample, drying overnight at 105 °C, and then weighing again to obtain dry weight (Givelet et al., 2004). Core data were examined for compression and/or expansion, but no mathematical corrections were needed. The soil monolith removed from the surface of Browns Island was corrected for expansion.

3.3. Plant processing

To remove as much sediment as possible, live roots and rhizomes, which are the main organic contributors to peat formation, were rinsed briefly in deionized water and blotted dry. Further cleaning involved immersing rinsed samples in deionized water and placing them in a vibrating disrupter/homogenizer (Vortex). This process was repeated until the deionized water ran clear. Balch tubes containing the samples were then filled with deionized water, placed in a sonic bath and sonicated at 51 kHz for 20 min. After particles settled for 1 h, samples were gently retrieved from the tubes and examined at 40× magnification for the presence of mineral particles. When particles were no longer observed, samples were freeze-dried for 12–24 h until all liquid was removed. Dried samples were stored in sealed vials until analysis.

3.4. Water salinity data

Surface-water salinity data for each of the marsh sites used for the plant study were obtained from long-term gauge stations monitored by the U.S. Geological Survey, the California Department of Water Resources, and the National Estuarine Research Reserve Program. Mean annual surface salinity values, data sources, years available, and long-term salinity trends are provided in Table 3.

3.5. Chemical analyses

The percentage of organic matter in dried bulk density samples was determined by standard loss on ignition procedures (Heiri et al., 2001) at 4-cm intervals near the top and bottom of each core and otherwise at 10-cm intervals. On average, duplicates were run every 9–10 samples. Reproducibility of duplicate analyses ranged from 0% to 4.8% with an average value of 0.74%.

Two-cm sections of core were frozen on dry ice and shipped to the USGS laboratory in Boulder, Colorado where they were freeze-dried and milled in polyethylene vials with acrylic balls using a SPEX® Model 8000 mixer mill. In the monolithic block from the BRI surface, inorganic (clay lenses) and organic material ("relatively pure peat") in 4 contiguous 2-cm sections ranging in depth from 0.220 to 0.171 m MSL were separated using a ceramic knife to compare the chemistry of these different components of the peat matrix.

Concentrations of Sr, U, Ti, Al, and Zr in freeze-dried peat and modern plant roots were determined by inductively coupled plasma mass spectrometry (ICP–MS) using a Perkin Elmer Elan Model 6000 and inductively coupled plasma atomic emission spectrometry (ICP-AES) using a Perkin Elmer Optima Model 3300DV. For these analyses, approximately 100 mg of solid material was completely dissolved in an HCl–HNO_3–HF acid mixture using a microwave total-digestion procedure (Roth et al., 1997; Barber et al., 2003; Hart et al., 2005). The digested samples were diluted at 1:10 (volume:volume, digest:water) with 18 MΩ cm deionized water and were preserved with distilled nitric acid. Aerosols of acidified aqueous samples were introduced into both spectrometers using a high-solids Burgener pneumatic nebulizer. Multiple internal standards covering most of the mass range (In, Ir, and Rh) were used to correct for system drift. Standard reference materials (SRM) from the National Institute of Standards and Technology (NIST) (Buffalo River Sediment, NIST SRM 8704 and Marine Sediment NIST SRM 2702) were digested and analyzed with each analytical batch. Additional details regarding the specific analysis techniques, procedures, and instrumental settings for ICP-MS analyses can be found in Garbarino and Taylor (1996) and Taylor (2001); and for ICP–AES in Garbarino and Taylor (1979), Boss and Fredeen (1999), and Hart et al. (2005).

All concentrations were determined in triplicate on a single digestion of each freeze-dried, homogenized sample. The standard deviation (sd) for the triplicate analyses was determined for each digest. In addition, replicate digestions were done every 10 samples to test homogeneity.

3.6. Sr and U isotope analyses

Isotopic compositions of Sr and U were determined in the USGS Denver Radiogenic Isotope Laboratory by thermal ionization mass spectrometry on a subset of the peat and plant digestions used for elemental analysis, and on samples of river water. Both Sr and U were chemically purified using ion chromatography (AG1 × 8 for U; Sr-Spec™ for Sr), loaded onto rhenium filaments (double assemblies for U; single filaments loaded along with tantalum oxide for Sr), and run on a Thermo Finnigan Triton multi-collector, thermal ionization, isotope ratio mass spectrometer.

Sr isotope ratios were determined in either static or multi-dynamic analytical mode, and $^{87}Sr/^{86}Sr$ atomic ratios were corrected for mass fractionation using $^{88}Sr/^{86}Sr$ measured in the same run. Reported $^{87}Sr/^{86}Sr$ values are also corrected for inter-laboratory bias by normalizing to the mean value obtained for Sr isotope standard NIST 987 analyzed along with samples and assuming a value of 0.710248 (McArthur et al., 2001). Replicate analyses of Sr in modern-marine carbonate standard, EN-1, run during this time gave a mean value of 0.709176 ± 0.000014 (2 × sd; $N = 48$) which is within error of the accepted value of 0.709174 ± 0.000002 for

Table 3
Surface water salinity data for gauges (deployed below mean lower low water at a 15-min timestep) in the San Francisco Estuary. All data were collected as salinity, except for Browns Island sites which were collected as specific conductance and corrected to salinity by multiplying by 0.0006364 (Ganju et al., 2005).

Site	Mean salinity (psu, (sd))	Source	Years available
Galinas Creek (San Pablo Bay)	23.2 (4.2)	San Francisco Bay National Estuarine Research Reserve under NOAA's National Estuarine Research Reserve System's (NERRS) National Monitoring Program	5/1/2008–12/31/2009
Rush Ranch (Grizzly Bay)	6.1 (2.0)	NERRS National Monitoring Program	5/20/2008–12/31/2009
Browns Island (the Delta)	1.8 (1.8)	Two USGS gauges: sites described in Ganju et al. (2005)	3/27/2002–5/20/2002; 11/9/2002–12/17/2002; 3/12/2003–4/16/2003; 9/5–28/2005; 10/12–26/2005; 1/11/2006–2/1/2006
Franks Wetland (the Delta)	0.7 (0.4)	SJO gauge of the California Department of Water Resources	1/1/2007–12/31/2008

modern seawater (McArthur et al., 2006). Delta values in per mil (‰) used in this report are calculated with the following equation: $\delta^{87}Sr = (({}^{87}Sr/{}^{86}Sr_{sample}/{}^{87}Sr/{}^{86}Sr_{seawater}) - 1) \times 1000$, using the ${}^{87}Sr/{}^{86}Sr_{seawater}$ value given above. Analytical errors determined by replicate analyses of standards and unknowns are better than ±0.00002 (= ±0.03‰ for $\delta^{87}Sr$) and represent 95% confidence levels (2 × sd).

U isotope ratios were determined in multi-dynamic peak-hopping mode using a single secondary electron multiplier. Ratios were corrected for mass fractionation using the known ${}^{236}U/{}^{233}U$ isotope ratio in an added double spike. Replicate analyses of U-isotope standard (NIST 4321B run between January 2009 and July 2010) yielded a mean ${}^{234}U/{}^{235}U$ atomic ratio of 0.0072921 ± 0.0000135 (= ±0.19% based on 2 × sd; $N = 134$), which is within analytical uncertainty of the accepted value (0.007294 ± 0.000028). Corrections for instrument drift were made by normalizing ${}^{234}U/{}^{235}U$ values measured for unknowns by the same factor needed to correct measured ${}^{234}U/{}^{235}U$ ratios for the SRM 4231B standard run in the same magazine. Measured ${}^{234}U/{}^{235}U$ atomic ratios were converted to ${}^{234}U/{}^{238}U$ activity ratios (AR) using decay constants published by Cheng et al. (2000) ($\lambda_{234} = 2.8262 \times 10^{-6}\ yr^{-1}$) and Jaffey et al. (1971) ($\lambda_{238} = 1.55125 \times 10^{-10}\ yr^{-1}$), assuming that all U has a ${}^{238}U/{}^{235}U$ composition of 137.88 (Steiger and Jäger, 1977). Replicate analyses of a solution of 69 million year old U ore (Ludwig et al., 1985) assumed to be in radioactive secular equilibrium were typically within analytical uncertainty of 1.000. However, the long-term average ${}^{234}U/{}^{238}U$ AR value of 0.9983 ± 0.0025 (2 × sd; $N = 93$) indicates a small systematic bias, implying that the ore "standard" may not completely satisfy the assumption of closed-system evolution. Analytical errors for measured ${}^{234}U/{}^{238}U$ AR values are given at the 95% confidence level (2 × sd) and include contributions from within-run uncertainties (counting statistics) plus uncertainties propagated from blank, spike, and mass fractionation corrections, as well as external error derived from multiple analyses of the U isotope standard.

3.7. Peat dating

Peat profiles were analyzed for ${}^{137}Cs$ in order to estimate the depth of the 1963 layer. The activities of ${}^{137}Cs$ in core sections within the top meter of peat were counted using a gamma detector (low-background germanium detector) and a multi-channel analyzer at USGS laboratories in Denver, CO and Menlo Park, CA. Samples were analyzed for 24–48 h to achieve the desired precision. This method has been used extensively to date peat and sediments in wetlands and lakes (Armentano and Woodwell, 1975; DeLaune et al., 1983; Ritchie and McHenry, 1990; Van Metre and Fuller, 2009). ${}^{137}Cs$ is a product of atmospheric fall-out from nuclear weapons testing and power plant accidents. Significant levels of this isotope first appeared in the atmosphere in the early 1950s, with peak quantities detected in 1963. The peat or sediment layer from 1963 can be identified based on the maximum activity of ${}^{137}Cs$ in a profile. It is important to note that there is some uncertainty about the long-term immobility of ${}^{137}Cs$ in peat due to processes such as diffusion and advection through porewater, uptake by vegetation, and flushing by waters of higher salinity (Turetsky et al., 2004; Foster et al., 2006). However, because research has shown lower mobility of ${}^{137}Cs$ in peat containing clay minerals (MacKenzie et al., 1997), which is the case in the Delta, and because we are most interested in variations on a millennial time scale, we decided that using ${}^{137}Cs$ dating to estimate the 1963 horizon satisfies the needs of this study. We estimated the location of the 1850 peat horizon, which represents the initiation of the California Gold Rush period, by examining peat geochemistry. Hydraulic gold mining, which began in 1852, resulted in a sharp rise in Pb and/or Hg contamination in the San Francisco Estuary (Hornberger et al., 1999; Alpers and Hunerlach, 2000; Domagalski, 2001; Bouse et al., 2010). Therefore, we identified this critical time period in California history by searching for major increases in Pb and/or Hg in the peat record. By normalizing these elements to Ti to account for variable sediment content (Alpers et al., 2008), we found rapid increases in Pb contamination beginning at approximately −0.153 (±0.12) m MSL at BRI, −0.29 (±0.04) m MSL at FW, and −0.17 m MSL at BACHI.

Radiocarbon dating of achenes (*Schoenoplectus* fruiting bodies), seeds, charcoal, and other terrestrial macrofossils were used to estimate ages greater than 250 years. Radiocarbon samples were analyzed by accelerator mass spectrometry at the Center for Accelerator Mass Spectrometry, Lawrence Livermore National Laboratory in Livermore, California. Ages were calibrated using CALIB (version 5.0.1; Stuiver and Reimer, 1993) with the INTCAL04 curve (Reimer et al., 2004). Age-depth spline fit models for the complete peat profiles (all 2-cm sections) were constructed following the procedure in Heegaard et al. (2005). Additional information about the ${}^{14}C$ dating of the peat cores, including all data, is reported elsewhere (Drexler et al., 2009a).

3.8. Three-component isotope ratio mixing models

Water in the Sacramento-San Joaquin Delta is derived from freshwater inputs from the Sacramento and San Joaquin Rivers and seawater from the San Francisco Estuary. Each of these sources has a distinct chemical and isotopic fingerprint. Therefore, the dissolved ion load in the water column at any given place will mostly consist of a mixture of these three sources, which reflect the ion concentrations of each end member. The $\delta^{87}Sr$ and ${}^{234}U/{}^{238}U$ AR compositions of the mixture depend on both the isotopic compositions and the Sr and U concentrations of end members. Because the isotopic compositions of these constituents are not strongly affected by near-surface chemical reactions or processes, simple binary mixing equations were used to describe the resulting $\delta^{87}Sr$ and ${}^{234}U/{}^{238}U$ AR compositions of the mixed water. The three-component mixing models employed in this study are based on theory and equations given in Faure (1986, chapter 9) and Faure and Mensing (2005, chapter 16).

In a system consisting of two end-member components, X and Y, the concentration of any element in the mixture, C_M, is dependent on the concentrations of that element in both end members, C_X and C_Y, and the fraction of mixing, f, such that

$$C_M = C_X f_X + C_Y(1 - f_X) \quad (1)$$

where $f_X = X/(X + Y)$ and varies from 0 to 1. Mixtures of the two components will result in points that define a straight line between the end-member compositions on plots of C_X versus C_Y that are directly proportional to the value of f (Supplemental Fig. 1a). However, the isotopic composition of the mixture, R_M, depends on both the isotope ratios of end members, R_X and R_Y, as well as their elemental concentrations such that

$$R_M = R_X C_X f_x + R_Y C_Y (1 - f_X) \quad (2)$$

Because values of R_M are most strongly influenced by the component with the higher concentration, mixing curves no longer define straight lines on plots of R_M versus C_M, but instead a family of hyperbolic curves whose degree of curvature depends on the difference in concentration between C_X and C_Y (Faure and Mensing, 2005, Fig. 16.5). Furthermore, mixing fractions defined by f are no longer distributed proportionally along the mixing curve, but are compressed toward the end member with the higher concentration (Faure and Mensing, 2005, Fig. 16.6). Binary mixtures of two elements (Sr and U) with different isotope ratios can be

treated in the same way using two sets of mixing equations. Values of $\delta^{87}Sr_M$ and $^{234}U/^{238}U$ AR_M for any given value of f will plot along the curve depending on values of Sr_X, Sr_Y, U_X, and U_Y.

Three-component mixing of $\delta^{87}Sr$ and $^{234}U/^{238}U$ AR between components X, Y, and Z, can be treated as a series of separate two component mixtures. If all three components are present, mixtures will plot within the polygonal space defined by three 2-component mixing curves between X–Y, X–Z, and Y–Z. To quantify proportions of each component, mixing webs can be calculated using the two-component mixing curves between intermediate end members consisting of the R_M and C_M determined at 0.1 intervals of f for mixtures along all three two-end member curves.

For this study, $\delta^{87}Sr$ and $^{234}U/^{238}U$ end members consist of compositions observed in seawater, the Sacramento River, and the San Joaquin River (Supplemental Fig. 1b). Values for the seawater end members were obtained from McArthur et al. (2006) and Delanghe et al. (2002). Data for the Sacramento River end member were obtained from water samples collected for this study and data available from the U.S. Geological Survey National Water Information System (NWIS). Data for the San Joaquin River end member were obtained from water samples collected for this study, NWIS, and Westcot et al. (1992). Values of $\delta^{87}Sr$ for river water determined in this study are similar to those reported by Ingram and Sloan (1992). For the purposes of this study, we assume that $\delta^{87}Sr$ and $^{234}U/^{238}U$ AR values of all water sources within the Estuary have remained relatively constant throughout the Holocene, which is justified as a first approximation because the lithogenic components of the watershed have not changed for well over 100,000 years (Ingram and Sloan, 1992).

4. Results

4.1. Proof of concept study

The results of the proof of concept study illustrate that the Sr isotopic compositions of modern plants reliably integrate the salinity signal throughout the Estuary. Sr and U concentrations and isotope data for *Schoenoplectus* roots/rhizomes are provided in Supplemental Table 1. $\delta^{87}Sr$ values in *Schoenoplectus* roots/rhizomes comprise a narrow range at each site, but a wider range between sites that is consistent with location within the Estuary (Fig. 2a). Seawater dominates $\delta^{87}Sr$ compositions at salinities above a few psu. Although the $\delta^{87}Sr$ composition of water present at each site was not measured, data for plants tend to follow the mixing relationship expected between seawater and freshwater represented by Sacramento and San Joaquin River water (solid and dashed curves in Fig. 2a). The hyperbolic nature of the mixing curves is the result of the non-linear effects when large differences in Sr concentration are present between the mixing end members. The observed pattern of $\delta^{87}Sr$ versus salinity in plants is very similar to a plot of surface-water salinity and $\delta^{87}Sr$ measurements shown by Hobbs et al. (2010).

In contrast, a similar plot of $^{234}U/^{238}U$ AR versus salinity shows that compositions of roots/rhizomes from Franks Wetland and Galinas Creek are broadly consistent with a mixing model involving seawater and freshwater from the Sacramento River. However, samples from Browns Island and Rush Ranch have much greater variations that deviate to higher values than those expected from simple mixing of seawater and freshwater (Fig. 2b). We note that roots/rhizomes with the highest $^{234}U/^{238}U$ AR values tend to have substantially lower U concentrations (~0.11 μg g^{-1} or less) than samples that conform to the salinity mixing pattern (typically >0.2 μg g^{-1}) or samples of peat from the Delta (median value of 3.8 μg g^{-1} for 150 analyses). We also note that U concentrations in roots/rhizomes with elevated $^{234}U/^{238}U$ AR are much lower than

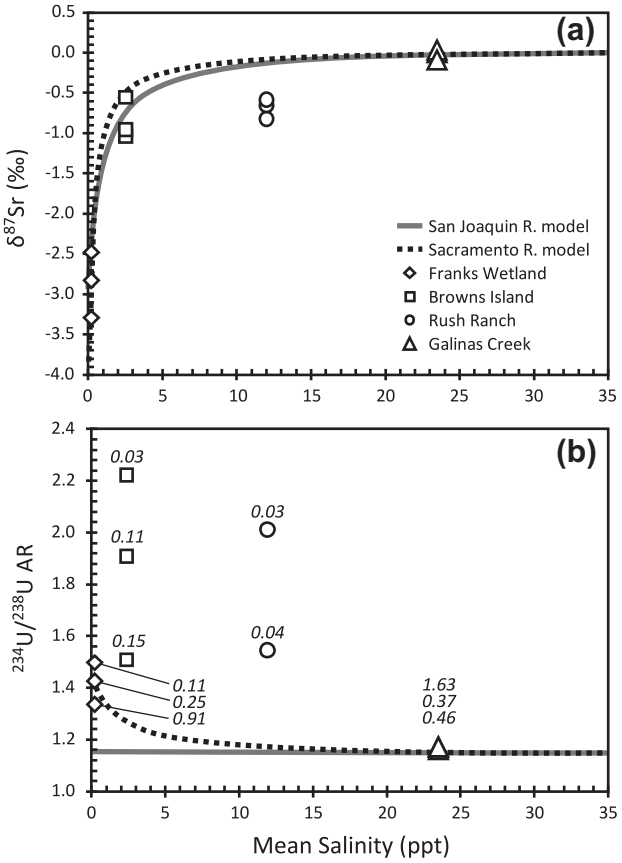

Fig. 2. Mean surface water salinity vs. (a) $\delta^{87}Sr$ and (b) $^{234}U/^{238}U$ activity ratio (AR) determined in living *Schoenoplectus* roots/rhizomes collected from four sites in the San Francisco Estuary representing a salinity gradient from fresh to saline marshes. Data are from Supplemental Table 1. Simple binary mixing models are shown for mixtures of seawater and Sacramento River water (dotted lines) and San Joaquin River water (solid lines) using data from Supplemental Table 3. Italicized numbers in (b) are U concentrations in root/rhizome tissue from Supplemental Table 1.

Sr concentrations (median value for 11 samples in Supplemental Table 1 is 15 μg g^{-1} for Sr), making them more susceptible to influence by factors other than simple mixing.

Unlike Sr isotopes, U isotopes can be fractionated as a consequence of recoil processes associated with alpha-decay of ^{238}U. During this process, ^{234}U is physically displaced from the location of the parental ^{238}U atom due to the ejection of the alpha particle (Kigoshi, 1971). The resulting ^{234}U decay products are more susceptible to mobilization than ^{238}U due to factors such as radiation-induced ionization and damage of the crystal lattice (Gascoyne, 1992; Chabaux et al., 2008; Porcelli, 2008). Direct implantation of recoil ^{234}U is particularly noticeable in situations where adjacent phases have high and low U concentrations (Neymark and Amelin, 2008), such as the case here with low U root/rhizome tissue growing in higher U peat. Direct implantation of recoil ^{234}U into root/rhizome tissue may be further enhanced because recoil distances increase substantially in low density materials (Chabaux et al., 2008). Roots/rhizomes from BRI and Rush Ranch are particularly susceptible to influence by this process because of their low U concentrations compared to root/rhizomes analyzed from FW and Galinas Creek. It is likely that all roots/rhizomes incorporate a limited amount of recoil-generated ^{234}U from the peat in which they grow in addition to soluble U derived from the overlying water column. However, at low concentrations, the addition of recoil ^{234}U may have a noticeable effect on the isotopic composition of U incorporated into the living root/rhizome tissue. Consequently, root samples with very low U concentrations are

likely to have $^{234}U/^{238}U$ AR values that are higher than values in the overlying water column.

4.2. Depth profiles in chemical and isotope data

Profiles of Sr and U concentrations show a large amount of scatter with time (or depth) at individual sites (Fig. 3a and b). This is particularly the case at Browns Island, which is located at the confluence of the two rivers. Correlation of short-term fluctuations is not readily apparent between sites. Furthermore, both Sr and U concentrations show substantial overlap between different locations within the Delta and do not clearly reflect a salinity gradient from BRI to BACHI.

In contrast, profiles of Sr and U isotopic compositions show less scatter over time and greater separation between sites (Fig. 3c and d). All peat samples have $\delta^{87}Sr$ compositions that range between values measured for Sacramento River water (−3.83‰) and seawater (0‰). Values for BRI peat samples are typically equal to or substantially higher than values observed in FW or BACHI samples, which is consistent with the greater contributions from seawater in the western Delta than further upstream.

Unlike $\delta^{87}Sr$, $^{234}U/^{238}U$ AR values for two of the three sources of water (San Joaquin River and seawater) are nearly identical (Fig. 3d). Values of $^{234}U/^{238}U$ AR for older peat samples clearly distinguish BRI from the two fresher sites, BACHI and FW (Fig. 3d). FW and BACHI samples plot closer to the value for San Joaquin River water and BRI samples plot closer to values for Sacramento River water. However, starting around 350 BCE, $^{234}U/^{238}U$ AR values in peat samples from BRI gradually decrease towards values observed in seawater and San Joaquin River water, reaching a low of ~1.15 at around 1850–1900 CE. During this time period, peat samples from FW and BACHI shift subtly toward Sacramento River composition in terms of both $^{234}U/^{238}U$ AR and $\delta^{87}Sr$.

4.3. Relationships with Ti content

There is a strong relationship between Ti and ash content in the peat from all three sites in the Delta (Fig. 4). This strong relationship justifies the use of Ti normalization to account for varying amounts of sediment being incorporated into the peat through time.

Plots of various elements vs. Ti suggest different processes by which elements have become incorporated into the peat matrix (Fig. 5). Because a pure organic component could not be isolated from peat samples prior to analyses, a means of discriminating between contributions from lithogenic and hydrogenic sources is needed. A number of elements are highly insoluble in typical surface water including Ti, Al, and Zr. The source for these elements is the inorganic sediment incorporated into the peat. This is evident in plots of Al and Zr versus Ti from peat samples at BRI (Fig. 5a and b) where all three elements define lithogenic mixing lines that pass through the origin as well as through clay-rich samples from either near the top of the profile or the basal clay. No additional source for these elements is required.

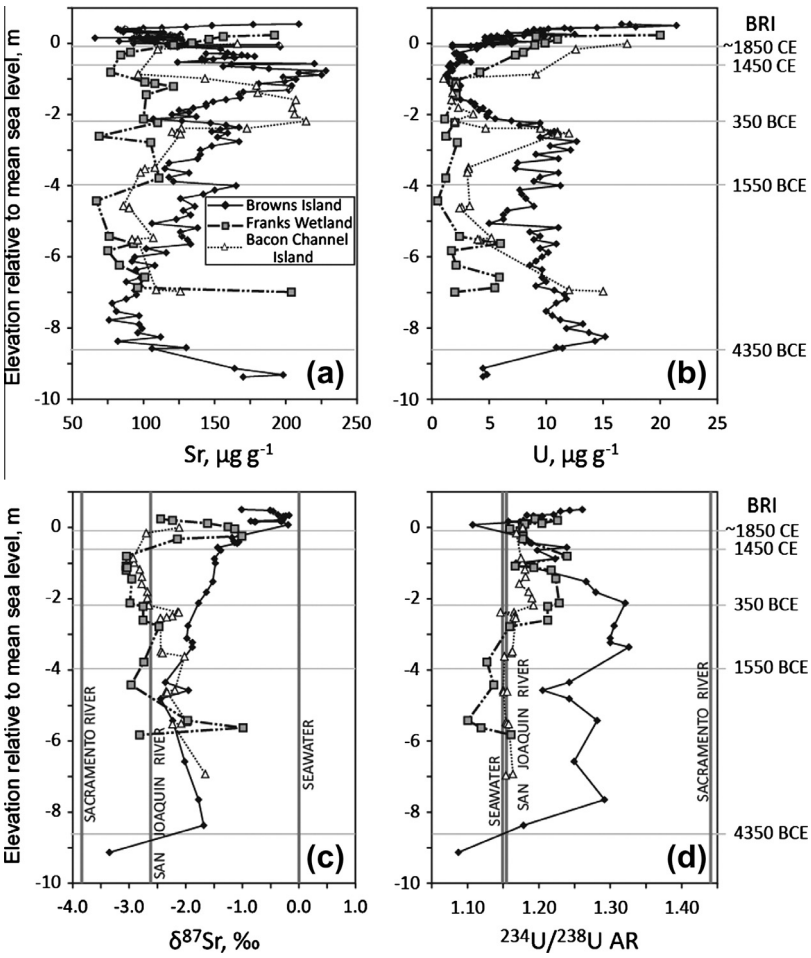

Fig. 3. Plots of Sr concentrations (a), U concentrations (b), $\delta^{87}Sr$ values (c), and $^{234}U/^{238}U$ AR (d) versus elevation relative to mean sea level (and peat age for BRI) in peat samples.

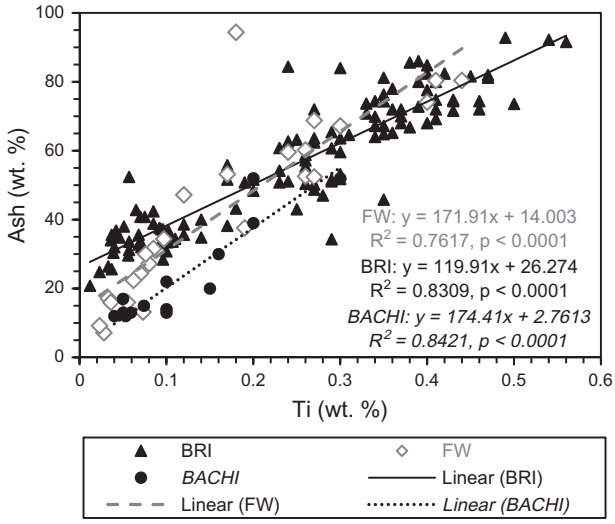

Fig. 4. Relationships between Ti concentrations and ash content of peat samples at BRI, FW, and BACHI.

The lithogenic source also contains some U and Sr; however, neither of these elements has a strong correlation with Ti as do Al and Zr (Fig. 5c and d). U concentrations of most peat samples are greater than values predicted by contributions from the lithogenic source based on Ti concentrations (i.e., they fall above the lithogenic mixing lines in Fig. 5c). The proportion of U derived from non-lithogenic sources (U_N) can be calculated by subtracting the U attributable to lithogenic sources (U_L) from the U measured in total digestions of peat samples (U_T). Values for U_N range from near 0% to 89%; however, median values of 55% and 73% are obtained depending on whether basal clay or clay-rich layers near the top of the profile are used to represent the lithogenic component. These results indicate that most of the U present in peat samples is derived from non-lithogenic sources.

Unlike U, Sr concentrations in peat samples show no relation to lithogenic mixing models and can have values either lower or higher than those expected based on Ti concentrations (Fig. 5d). Furthermore, peat samples show a crude negative correlation between Sr and Ti (gray band in Fig. 5d). These relations indicate that lithogenic Sr does not provide a significant contribution to peat samples despite similar concentrations in peat and clay-rich samples. Instead, samples of clay-rich materials may be contaminated with small amounts of organic matter that contribute much of the Sr in the bulk analysis.

These data indicate that Sr and U in peat samples are not particularly sensitive to contributions from inorganic sediment included in the peat matrix. Unlike Ti, both U and Sr are soluble in oxidizing surface waters including seawater and river water. Therefore, it is likely that variations observed in these elements are due to shifts in contributions from multiple hydrogenic sources. Minimal influence by lithogenic components in Delta peat samples is further supported by isotope data. Four of the five samples of clay-rich material from BRI have measured $^{234}U/^{238}U$ AR values that are lower than those observed in peat (Fig. 6a). These results are consistent with the concept that most lithogenic source material is old enough to have reached radioactive secular equilibrium ($^{234}U/^{238}U$ AR = 1.0). However, the fact that all clay-rich samples have $^{234}U/^{238}U$ AR values greater than 1 indicates a strong likelihood that the fine sediment constituting the lithogenic faction

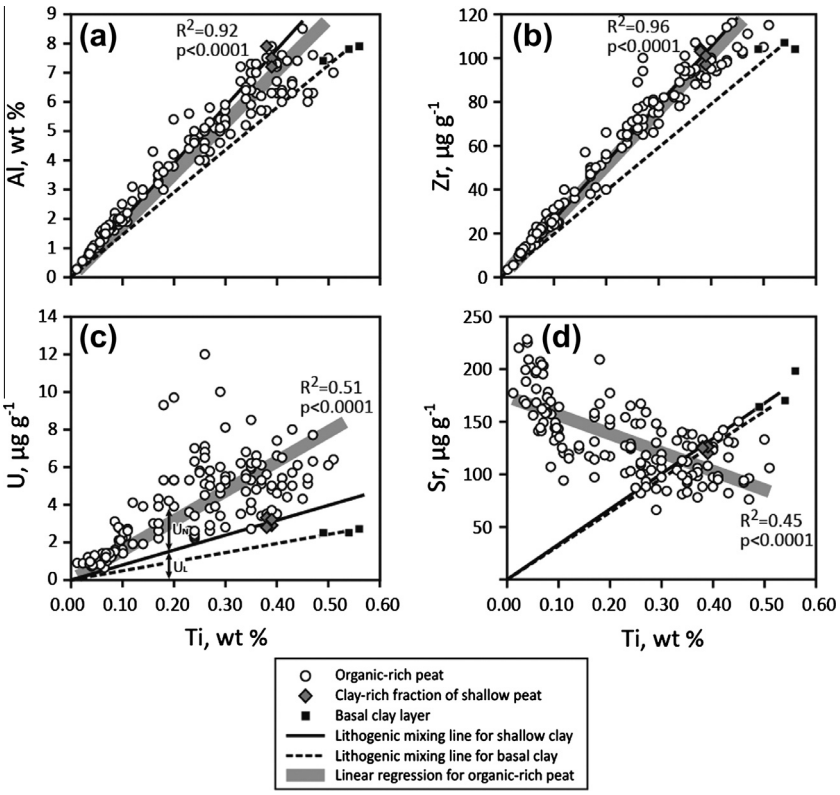

Fig. 5. Relationships between Ti concentrations and aluminum (a), zirconium (b), uranium (c), and strontium (d) at BRI. Lithogenic mixing lines are shown for plots of concentration and are based on the assumption that clay-rich materials represent the lithogenic component of peat samples and that concentrations attributable to the lithogenic component are zero when Ti is zero. R^2 and p-values provided for simple linear regressions for organic-rich peat (thick gray lines). See text for explanation of U_N and U_L in (c).

includes U adsorbed from the water in which it was transported. The sorption capacity of fine clays, ferrihydroxides and amorphous silica, can vary from minimal to substantial depending on mineralogy and grain size as well as physical conditions and chemical compositions of the fluids (Borovec, 1981; Ames et al., 1983; Andersson et al., 2001; Chabaux et al., 2003, 2008). U adsorption onto surfaces of fine, inorganic particles during transport further decouples the connection between lithogenic and hydrogenic sources for U. Consequently, values calculated for U_L likely include a substantial component of U_N whose $^{234}U/^{238}U$ AR is more likely to reflect the composition of the hydrogenic source rather than the original lithogenic source from which Ti is derived. This scenario is supported by the lack of a correlation between $^{234}U/^{238}U$ AR and Ti in peat samples that would be required if the lithogenic fraction made a significant contribution to U_T (Fig. 6a). Likewise, $\delta^{87}Sr$ values in peat do not show an overall correlation with Ti, although samples do show an intriguing V-shaped pattern that reflects changes in both Ti and $\delta^{87}Sr$ with time (Fig. 6b). Variations in these constituents shift more or less systematically throughout the entire 6000+ year period of Delta evolution (see profile in Fig. 3c). Thus, they cannot reflect simple mixing trends between lithogenic and non-lithogenic components at any given time and more likely reflect evolving depositional and environmental conditions.

4.4. Paleosalinity mixing model based on Sr–U data

The results of simple mixing in Sr–U concentration space can be represented by an ordinary ternary plot (Supplemental Fig. 1a), however in $\delta^{87}Sr$–$^{234}U/^{238}U$ AR space, the ternary plot becomes warped and stretched due to the large differences in Sr and U concentrations between end members and the non-linear nature of mixing relations (Supplemental Fig. 1b). Mixtures of the three end members are greatly influenced by addition of seawater because of its relatively high concentration of Sr. Addition of as little as 10% seawater causes $\delta^{87}Sr$ to increase from low values in freshwater sources (−2.62‰ to −3.84‰ for San Joaquin and Sacramento River water, respectively, Supplemental Fig. 1a) to values as high as −0.35‰. Furthermore, the large difference in U concentration between the two rivers (0.13 and 5.0 μg l^{-1} for Sacramento and San Joaquin River water, respectively, Supplemental Fig. 1b) results in substantial variation in $^{234}U/^{238}U$ AR values even if water in the Delta remains dominated by freshwater sources. Mixtures of up to 20% San Joaquin River and 80% Sacramento River waters can be readily discriminated; however, once the Sacramento River component drops to less than about 70%, $^{234}U/^{238}U$ AR in mixed water becomes dominated by U from the San Joaquin River, obscuring further quantification.

Because Sr and U present in peat samples are dominated by hydrogenic rather than lithogenic components, isotopic compositions of whole peat digestions should reflect mixtures of the three main water sources within the Delta. Nearly all peat samples representing different time periods in the Delta fall within or very close to the distorted 3-member mixing triangle (Fig. 7). Samples that fall outside the limits of the mixing model consist of one of 37 peat samples from BRI (from the ~1850 to 1963 period), all the clay samples from BRI (which are dominated by lithogenic rather than hydrogenic components), and 4 of 23 FW peat samples (Fig. 7b and c). Peat samples from BACHI show the tightest cluster of $\delta^{87}Sr$ and $^{234}U/^{238}U$ AR values, probably because this site is geographically the least likely to be influenced by hydrologic inputs from either seawater or Sacramento River water. Peat samples from FW show substantially greater scatter, consistent with its position closer to both seawater and Sacramento River sources. $\delta^{87}Sr$ compositions indicate that seawater was a minor constituent remaining < ~5% throughout the last 6000 years. Variations in U isotopes in FW peat indicate that freshwater sources fluctuated greatly, alternating between domination by the San Joaquin vs. the Sacramento River (Fig. 7c). Peat samples from BRI show the greatest amount of variability between freshwater sources because of its position at the confluence of both rivers and the greatest influence from seawater due to its location at the western (seaward) boundary of the Delta (Fig. 7b).

Over time, there is considerable variability in $\delta^{87}Sr$ and $^{234}U/^{238}U$ AR in BRI peat samples (Fig. 7b), which can be related to changing patterns of paleosalinity in the Delta. The oldest peat samples (4350–1550 BCE shown by black symbols) have the lowest $\delta^{87}Sr$ values and likely represent conditions with the least seawater (a mean of approximately 1%, which is equivalent to ~0.35 psu). These samples show a wide range of $^{234}U/^{238}U$ AR values and may represent frequent shifts between the San Joaquin and Sacramento Rivers providing the dominant source of dissolved ions to the site. During the period from 1550 to 350 BCE (dark blue symbols), samples cluster around $\delta^{87}Sr$ of −2.0, which is very close to the mean salinity of the oldest (black) group of samples. These samples also have $^{234}U/^{238}U$ AR values between 1.30 to 1.35 and plot close to the mixing line between seawater and Sacramento River water, indicating that the Sacramento River dominated the freshwater component during this time. Peat deposited during

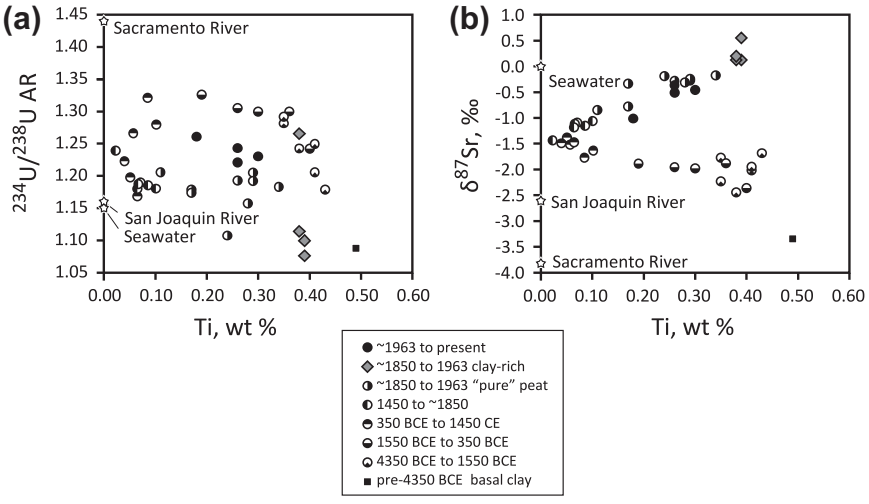

Fig. 6. Relationships through time between Ti concentrations and $^{234}U/^{238}U$ activity ratio (a) and $\delta^{87}Sr$ (b) in peat samples from BRI.

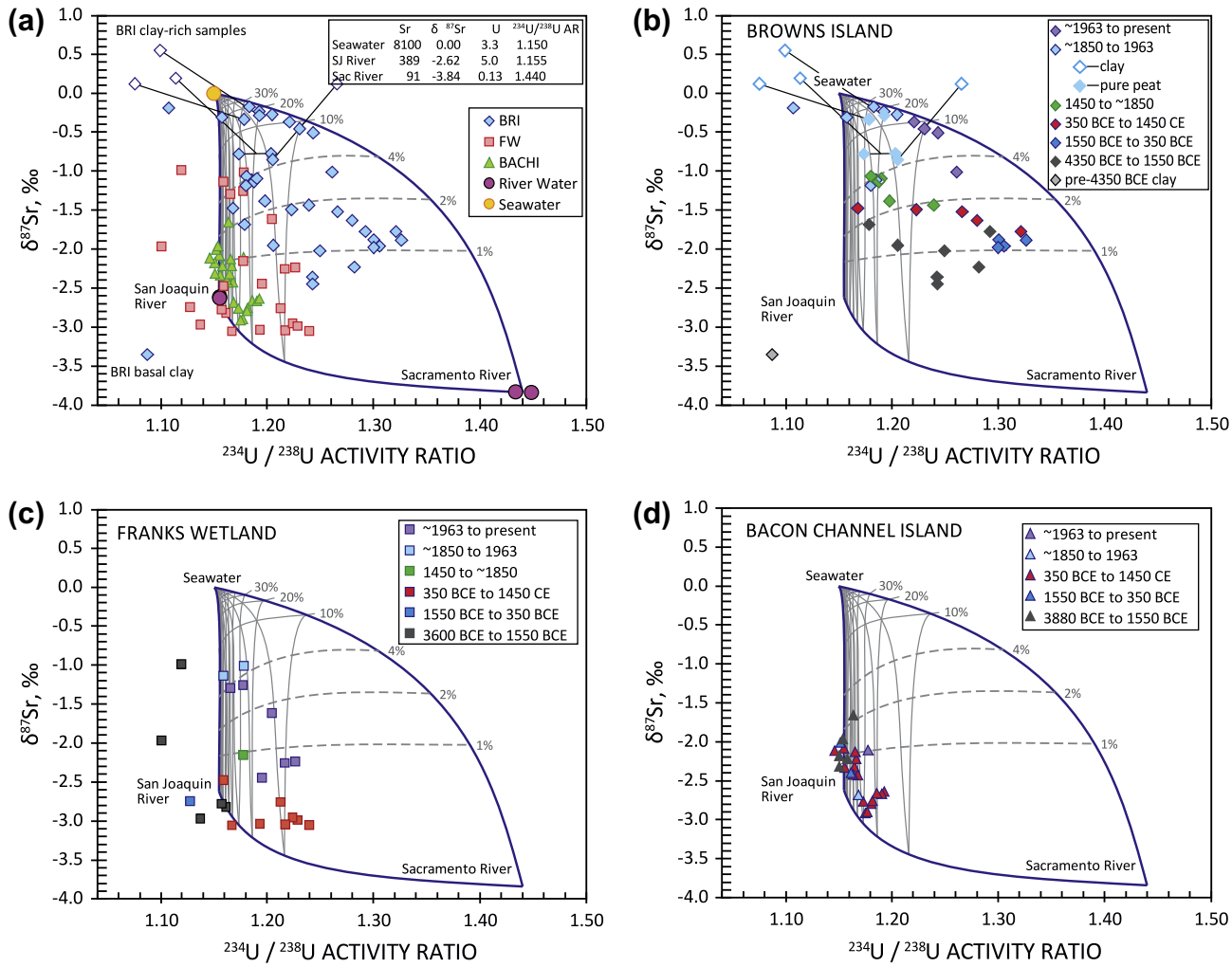

Fig. 7. Peat samples from all sites (a), BRI (b), FW (c), and BACHI (d) in $\delta^{87}Sr$–$^{234}U/^{238}U$ AR space with end members shown at the vertices of the distorted triangle. Source water isotopic compositions and concentrations ($\mu g\,l^{-1}$) for all three end members are provided in (a). In the individual site plots, age ranges (see Table 4 for peat depth ranges for each age category) are provided showing how the relative contribution of each end member has either changed or remained relatively constant through time. Gray lines indicate compositions for 30%, 20%, 10%, 4%, 2%, and 1% mixing intervals. The symbol "~" used before 1850 and 1963 age horizons indicates that there is a higher level of uncertainty in these dates relative to others used in the study. For BACHI, no data were available for the time period from 1450 to ~1850 CE.

350 BCE to 1450 and between 1450 and ~1850 (red and green symbols, respectively, in Fig. 7b) show a gradual shift toward lower $^{234}U/^{238}U$ AR and higher $\delta^{87}Sr$, implying progressive increases in contributions from the San Joaquin River from only a few percent to between 20% and 30% and seawater from about 1% to approximately 4% (~1.4 psu). During the period from ~1850 to ~1963 at BRI (light blue symbols in Fig. 7b), elevated $\delta^{87}Sr$ values imply that seawater was more important than previous periods. The most recent (purple) peat samples representing the period from 1963 to present (purple symbols) show a systematic progression of decreasing influence from both seawater and San Joaquin River sources.

Peat samples from FW show less $\delta^{87}Sr$–$^{234}U/^{238}U$ AR variability than BRI samples as well as a different pattern through time (Fig. 7c). During the period from 3600 BCE to 1550 BCE (black symbols) and from 1550 BCE to 350 BCE (dark blue symbols), several peat samples have compositions that fall very close to the San Joaquin River end member (two are slightly outside of the $\delta^{87}Sr$ – $^{234}U/^{238}U$ AR mixing model), suggesting that nearly all the water from FW was derived from that source. Two other peat samples from the older age group plot further to the left of the seawater-San Joaquin mixing line, suggesting that simple mixing of hydrologic sources is inappropriate for these samples. These two samples with $\delta^{87}Sr$ compositions of approximately −1.0 and −2.0 have lower concentrations of organic matter (loss on ignition = 31% and 64%, respectively) than most other samples and therefore contain greater amounts of lithogenic components compared to the average value at FW (Table 2). Incorporation of lithogenic sediment, especially material with lower clay or ferrihydroxide contents, is likely to drive $^{234}U/^{238}U$ AR toward lower values between 1.16 (dissolved U in San Joaquin River water) and 1.0 (secular equilibrium value). Values of $\delta^{87}Sr$ for rock components depend on $\delta^{87}Sr$ values of sediment sources in the watershed; however, values of −1‰ to −2‰ are consistent with pre-1850 CE sediment from a core collected in San Francisco Bay (Table 2 of Bouse et al., 2010). During the period from 350 BCE to 1450 CE (red symbols in Fig. 7c), the relative proportion of Sacramento River water increased to over 90%, while the proportion of seawater remained <1% (<0.35 psu). Only one peat sample represents the period from 1450 to ~1850 CE (green symbol) and, like BRI, it contains a slightly higher $\delta^{87}Sr$ value consistent with a small increase in seawater contribution (~1% or ~0.35 psu) relative to older peat samples. Similar to BRI, FW samples deposited during the ~1850 CE to ~1963 CE period (light blue) appear to have the

largest contributions from seawater (up to nearly 5%). Also like BRI, peat deposited at FW during the most recent (purple) period has $\delta^{87}Sr$–$^{234}U/^{238}U$ AR compositions similar to pre-1850 CE values.

At BACHI, the pattern through time is quite different from FW and BRI (Fig. 7d). Overall, the BACHI samples are closely tied to the signature of the San Joaquin River and have a very limited range in isotope values from −3.0‰ to −1.7‰ for $\delta^{87}Sr$ and from 1.14 to 1.18 for $^{234}U/^{238}U$ AR (Fig. 7d). However, there are some peat samples from 350 BCE to 1450 CE (red symbols) and a peat sample from ~1850 to ~1963 CE (light blue symbol) that indicate greater contributions from the Sacramento River. Variations in isotopic composition during the period from 1450 CE to ~1850 CE remain unknown because no samples from this age range were available from the core. Overall, the seawater component at BACHI remained at 2% or less, with the predominance of samples plotting at 1% or less (<0.35 psu). The outlier at approximately 2% seawater (~0.7 psu) during the oldest period suggests a period of extremely low flow in the San Joaquin River.

5. Discussion

5.1. Paleosalinity tracers

In this study we used a combination of Sr and U concentrations and isotopic compositions in seawater, Sacramento River water, and San Joaquin River water to construct a three-end-member mixing model for the purpose of determining Delta paleosalinity (Fig. 7). The success of this approach was strongly tied to the provenance of the elements we used and how they came to reside within the peat matrix. For a tracer to effectively track salinity in peat, it must be derived from hydrogenic sources and reflect the composition of the water column at the time peat was formed. It must also be incorporated into the peat deposit and remain unmodified by post-depositional exchange with younger pore water (López-Buendia et al., 1999).

We found that Sr occurs in relative abundance in both the living plant tissue (~6 to 71 μg g^{-1}, median of 15 μg g^{-1}; Supplemental Table 1) and in the organic component of the peat (median of 125 μg g^{-1} for 200 peat samples, Supplemental Table 4). The higher concentrations observed in peat samples are interpreted as the consequence of decay and compaction of the original organic matter. Although a certain amount of secondary mobility of Sr may have occurred during and after peat formation, a number of factors imply that such exchange is not of major consequence in this study. The crude negative correlation between Sr and Ti concentrations (Fig. 5d) indicates that Sr resides primarily in the organic fraction of the peat and is derived from hydrogenic rather than lithogenic sources. The substantially higher Sr concentrations present in living roots compared to fresh water sources (up to 24 μg g^{-1} in *Schoenoplectus* spp. roots from FW compared to 0.39 μg g^{-1} in San Joaquin River water; Supplemental Tables 1 and 3) reflects the ability of these plants to selectively incorporate Sr along with other nutrients. The similarity of $\delta^{87}Sr$ values in living plant tissue and ambient water (Fig. 2a) is consistent with incorporation by plants of dissolved Sr from surface water rather than from older peat or mineral sources. Samples of pore water were not analyzed in this study; however, the much lower Sr concentrations in surface water within the Delta (mixtures of river water and seawater between 0.09 and 8.1 μg g^{-1}) would not be able to readily alter the composition of peat without large water to peat volume ratios. This is unlikely given the low hydraulic conductivity of tidal marsh soils (Rabenhorst, 2001), the low tidal fluctuations in this part of the Estuary, and the absence of the hydraulic head needed to drive flow through peat deposits that are near or below sea-level elevations. Furthermore, release of any Sr during decomposition would not affect $\delta^{87}Sr$ compositions remaining in the peat. These factors, plus the preservation of systematic variations in $\delta^{87}Sr$ values in peat profiles (Fig. 3), are strong evidence of primary, rather than secondary, causes for the observed Sr isotopic compositions.

U concentrations are much lower than Sr in living plant tissue (0.03–1.63 μg g^{-1}, median of 0.15 μg g^{-1}; Supplementary Table 1) and, therefore, living plants likely contribute only a small part of the total U budget in peat samples. Concentrations of U in peat (median value of 3.7 μg g^{-1} for 200 analyses; Supplemental Table 4) are more than three orders of magnitude higher than values in oxidizing surface waters (0.00013–0.005 μg g^{-1}; Supplemental Table 3). Much of the U that becomes incorporated into the peat

Table 4
Age categories and corresponding depth ranges in peat cores from BRI, FW, and BACHI. Full ^{137}Cs data are provided in Supplemental Table 2. Sources for radiocarbon dating and determination of the ~1850 horizon are described in the text.

Site	Age category	Depth range (measuring from bottom of each 2-cm section, m MSL)
BRI	~1963 to present[a]	0.330–0.490 (peat surface)
	~1850 to ~1963	−0.153 to 0.329
	1450 (T_{sd}[b] = 100) to ~1850	−0.680 to −0.154
	350 BCE (T_{sd} = 143) to 1450 CE	−2.280 to −0.681
	1550 BCE (T_{sd} = 100) to 350 BCE	−4.160 to −2.281
	4350 BCE (T_{sd} = 120) to 1550 BCE	−8.670 to −4.161
	Pre-4350 BCE	Deeper than −8.671
FW	~1963 to present	0.050 to 0.250 (peat surface)
	~1850 to ~1963	−0.290 to 0.049
	~1450 (T_{sd} = 130) to ~1850	−0.740 to −0.291
	350 BCE (T_{sd} = 100) to 1450 CE	−2.90 to −0.741
	1550 BCE (T_{sd} = 50) to 350 BCE	−4.30 to −2.91
	3600 BCE (T_{sd} = 125) to 1550 BCE	−5.83 to −4.31
BACHI	~1963 to present	0.010 to 0.210 (peat surface)
	~1850 to ~1963	−0.170 to 0.009
	1450 (T_{sd} = 60) to ~1850	−0.213 to −0.171
	350 BCE (T_{sd} = 100) to 1450 CE	−2.80 to −0.214
	1550 BCE (T_{sd} = 65) to 350 BCE	−4.43 to −2.801
	3880 BCE (T_{sd} = 90) to 1550 BCE	−7.05 to −4.431

[a] Dating for both the 1963 and 1850 horizons, which were determined with single event markers (^{137}Cs and geochemistry, respectively), has uncertainty that is difficult to quantify and for this reason is designated with "~".

[b] Error estimates for radiocarbon dates (1450 CE and older) are the total standard deviation, T_{sd}, assigned to each section of the entire core following Heegaard et al. (2005). T_{sd} incorporates an error estimate for each individual object (within-object variability of dated macrofossils) and for how representative each dated object is in relation to the sampled layer (between-object variability).

matrix does so as a result of its redox chemistry. Under the reducing conditions common in tidal marsh soils (Gambrell and Patrick, 1978; Rabenhorst, 2001), U drops out of water that flows over the marsh surface and is held tightly by organic matter in its highly insoluble U^{4+} state (Szalay, 1964; Idiz et al., 1986; Johnson et al., 1987; Owen et al., 1992; Zielinski et al., 2000; Swarzenski et al., 2003; McKee, 2008; Novak et al., 2011). Non-organic sources of U may also include contributions from the fine-grained sediments included in peat, although much of this "lithogenic" U may have been adsorbed onto reactive particle surfaces during its transport through estuarine waters (Andersson et al., 2001; Chabaux et al., 2003, 2008). As a consequence, "lithogenic" U (defined by its correlation with Ti) would likely have an isotopic composition that is similar to hydrogenic U. Once sequestered in anoxic peat deposits, U is not likely to become remobilized due to its very low solubility in reducing porewater. Therefore, U in peat samples, like Sr, is considered to have a predominately hydrogenic origin reflecting the mixture of freshwater and seawater components present at the soil–water interface at the time of peat formation. Just like the $\delta^{87}Sr$ data, U isotopic compositions demonstrate consistent behavior that independently shows similar variations in salinity over the same time periods (Fig. 3c and d). The available data and specific physical and geochemical conditions inherent in marshes in the Delta provide strong evidence that both Sr and U isotopic compositions of peat samples reflect variations in primary hydrologic components present at each site at the time of peat formation.

Despite the conclusion that Sr and U are both potentially useful hydrologic tracers, *concentrations* of these elements alone ultimately proved unsuccessful in tracking salinity (Fig. 3). This is likely because, under near-surface conditions, a variety of chemical reactions and physical processes can result in non-conservative behavior such as changes in state, concentration due to evaporation or plant transpiration, dilution by rainwater, precipitation of minerals from saturated solutions, dissolution of previously formed solids, and absorption or desorption from mineral or organic matter (Peros et al., 2007; Faure and Mensing, 2005). In contrast, isotope ratios of Sr and U are largely unaffected by these near surface processes, and, therefore, are better suited as tracers of water sources. Unlike isotopes of lighter elements (e.g., ^{18}O and ^{16}O, ^{13}C and ^{12}C), isotopes of Sr and U do not fractionate significantly during natural chemical reactions or physical transformations (Faure and Powell, 1972; Hart et al., 2004). The isotopic compositions of both U and Sr in the ocean are largely uniform worldwide due to the long residence times of these elements (U: 300,000–500,000 yrs; Dunk et al. (2002); and Sr: 2,500,000 yrs, Hodell et al. (1990)), making them highly conservative tracers for salinity. In contrast, the isotopic values of Sr and U in freshwater reflect the specific geology of the drainage basin and climatic factors (Faure and Mensing, 2005).

In the modern Sacramento-San Joaquin Delta, values of $\delta^{87}Sr$ are distinct for all three water sources (Supplemental Table 3). Although $^{234}U/^{238}U$ AR values for seawater and Sacramento River water are very distinct, $^{234}U/^{238}U$ AR values for San Joaquin River water and seawater are, by coincidence, almost indistinguishable. Consequently, contributions from these two sources cannot be determined on the basis of U isotopes alone. However, when used in combination with $\delta^{87}Sr$ values, $^{234}U/^{238}U$ AR are a highly effective tracer of the relative contributions of Sacramento and San Joaquin River water as long as seawater contributions remained low.

The basic assumption of our approach, that the salinity signal in peat tracks ambient salinity conditions, was confirmed by our proof of concept study, which showed that $\delta^{87}Sr$ compositions of *Schoenoplectus* roots/rhizomes vary consistently with salinity in the San Francisco Estuary (Fig. 2). Results of the proof of concept study are also consistent with $^{234}U/^{238}U$ results in roots/rhizomes, but only in those with higher U concentrations (see explanation in Proof of Concept Study section). However, live plants only contribute small amounts of the total U; most U in peat deposits originates from U in the water column that becomes tightly bound to peat under the reducing conditions typically found in tidal marshes (Rabenhorst, 2001; Swarzenski et al., 2003). Furthermore, even the U included in the lithogenic component, determined through its relationship with Ti, is likely to include a substantial component of hydrogenic U adsorbed on reactive particle surfaces during transport. Therefore, we conclude that $^{234}U/^{238}U$ AR measured in peat deposits should accurately reflect the isotopic composition of U in the water column at the site of deposition and that the isotopic composition of U is related to salinity by the uniform and well known $^{234}U/^{238}U$ AR of the seawater component (Supplemental Fig. 1). It is simply because of the coincidental composition of the seawater and San Joaquin end members that this tracer does not uniquely define salinity. Finally, we consider the excellent agreement between Sr and U isotope compositions in nearly all peat samples analyzed in this study (save the clay-rich samples) and the limits of three component mixing models based solely on compositions of aqueous end-members to be compelling evidence that these isotopes have reliably recorded the evolution of water within the Sacramento-San Joaquin Delta over the last 6000+ years.

5.2. 1850 CE – 1963 CE time period

Isotope data in this study imply that a major excursion toward the seawater end member occurred at approximately 1850 CE at both BRI and FW (Figs. 3c and d, 7b and c). This could be due to several factors. An intrusion of salinity could have occurred as a result of drought. Such intrusions took place in the 1930s, late 1980s and early 1990s, but data in Fig. 7b and c also show a freshening during the most modern period, which cannot be substantiated because higher freshwater flows did not occur during this period (The Bay Institute, 2003). Another possible cause for heightened salinity could be the construction of dams in the watershed. The damming of most of the major tributaries flowing into the Sacramento and San Joaquin Rivers began in the late 1800s and continued through the 1900s (California Department of Water Resources Division of Safety of Dams, 2009). However, this timing does not coincide with the apparent major seawater excursion because the largest dams, which could have altered the salinity regime in the Delta, were built in the 1940s through the 1970s. In 1994, a new management policy (X_2) was initiated in which surface water salinity 81 km upstream of the mouth of the San Francisco Estuary was actively managed not to exceed 2 psu (Kimmerer, 2002). Although such management has resulted in major changes in Delta ecosystems, it still cannot explain the pattern in the $\delta^{87}Sr$ data, which began in ~1850.

The California Gold Rush period, which started in 1849, has had a huge impact on many geochemical and geomorphological processes in the Estuary. Hydraulic mining, which occurred primarily during 1852–1884, liberated approximately 300 million tons of sediment mainly into the Sacramento River watershed (Gilbert, 1917; Bouse et al., 2010). Heavy metal contamination from this period is well documented in bay muds and peat (Hornberger et al., 1999; Domagalski, 2001; Bouse et al., 2010). In addition, during this period, progressive denudation of riparian forests and initiation of agriculture within the Sacramento River watershed increased downstream erosion and sediment supply (Gilbert, 1917; Florsheim and Mount, 2003). The slug of sediment deposited in San Pablo Bay sediments subsequent to the hydraulic mining period had a $\delta^{87}Sr$ signature of between −0.67‰ and 1.58‰ ($^{87}Sr/^{86}Sr$ values of 0.7087–0.7103), which is higher than pre-mining sediments ranging from −2.37‰ to −0.82‰ (Bouse et al., 2010). This large slug of sediment not only contributed directly to the suspended sediment load in the Estuary, but may have also

influenced the dissolved Sr load in estuarine waters, which was incorporated into the organic component of the peat. The samples from 0.351 to 0.065 m MSL in the BRI profile are within the 0.7087–0.7103 $^{87}Sr/^{86}Sr$ range (for peat and/or clay lens samples, see Supplemental Table 4). Therefore, they were likely influenced by anthropogenic activities during the Gold Rush period, particularly a sample from the ~1850 CE to ~1963 CE period (light blue marker) with approximately −0.2 $\delta^{87}Sr$ that appears outside U and Sr isotope space (Fig. 7b). These observations suggest that the movement of $\delta^{87}Sr$ in Delta peat samples toward the seawater end member may reflect the addition of radiogenic Sr from Gold Rush sources rather than a major increase in salinity. The most recent time period represents a recovery of the hydrologic system toward pre-mining values. Additional investigations are required to fully explain the causes for the observed isotopic anomaly during this period of exceptionally rapid landscape change.

At FW, increases in $\delta^{87}Sr$ values of two peat samples (0.44 and 0.30 m MSL; light blue markers in Fig. 7c) during the Gold Rush period are not as great as those at BRI. The smaller increases are likely related to the location of the site further upstream in the Estuary, and further away from the influence of the Sacramento watershed where most mining activities were focused. Similar to BRI, peat samples from the modern period (purple markers) represent a recovery to $\delta^{87}Sr$ values before the Gold Rush period. At BACHI, no such pattern of increased $\delta^{87}Sr$ in young peat samples is observed (Fig. 7d). Lack of variation at BACHI is likely due to its location even further upstream in the San Joaquin River basin away from both tidal fluxes and sources of mining sediment transported mostly through the Sacramento River.

5.3. Delta paleosalinity within the context of the estuary

A wide range of paleosalinity research has been conducted in the San Francisco Estuary, west of the Delta. Much of it has been aimed at understanding long-term variability in climate and its influence over mean annual freshwater discharge in the watershed (e.g., Ingram et al., 1996; May, 1999; Stahle et al., 2001; Malamud-Roam and Ingram, 2004), which largely determines the salinity regime of the Estuary (Peterson et al., 1989). The long-term paleosalinity reconstructions fit the expected trend of high salinity near the mouth of the Estuary (South and Central Bays) and decreasing salinity with distance upstream (Suisun Bay > the Delta). This pattern has not changed greatly over the past 6000+ years (Fig. 8). The South and Central Bays have been polyhaline during much of the record (Ingram and DePaolo, 1993) (salinity scale based on Cowardin et al. (1979), Fig. 8). The Suisun Bay has varied between mesohaline and oligohaline, with a freshening during the past 500 years. Beginning in 1930 or so, however, an increase in salinity was observed, which was likely the result of upstream dam-building and water diversion for the California State Water Project and the Federal Central Valley Project (Byrne et al., 2001).

The Delta, which is the landward most part of the Estuary, has long been considered a tidal freshwater marsh region (e.g., Weir, 1950; Shlemon and Begg, 1975; Prokopovich, 1988; Rojstaczer et al., 1991; Ingebritsen et al., 2000). The data presented here demonstrate that, of the three study sites, BACHI and FW have been mainly fresh over the past 5000+ years (Fig. 8). However, the results from BACHI show rare spikes of salinity, during which conditions changed from fresh to oligohaline (between 3880 and 1550 BCE; Fig. 7d). Such spikes in salinity likely occurred during major droughts in the region. The overall salinity pattern suggests that any points upstream of BACHI would also have been mainly fresh for the past 5000+ years. Although the freshwater status of BACHI is largely tied to the San Joaquin River, there have been periods when discharge from the Sacramento River was important (particularly from 380 CE to 1450 CE, red markers with $\delta^{87}Sr < -2.6$; Fig. 7d). This could have been due to periods of flooding, when flows from the Sacramento River overwhelmed the

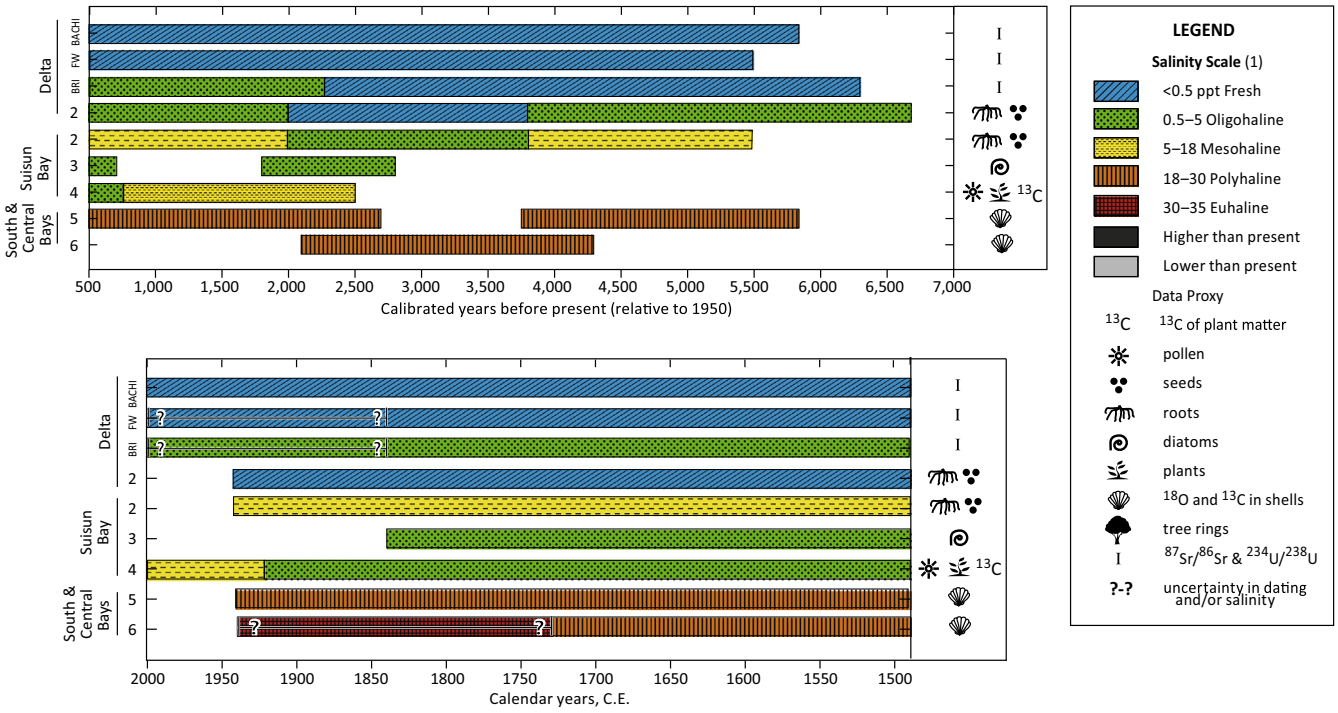

Fig. 8. Major paleosalinity trends in the San Francisco Estuary based on this study and the literature. Only studies with long-term, quantified trends that were well-dated are included. The vertical axis represents different parts of the San Francisco Estuary in which distance from the Golden Gate increases according to South and Central Bays < Suisun Bay < Delta. Panel (I) shows 7000 through 500 calibrated years before present (relative to 1950, which is "present" for radiocarbon dating) and Panel (II) shows 1450 CE through 2000 CE. The numbers on the legend and y-axes refer to the following references: (1) Cowardin et al. (1979), (2) Goman and Wells (2000), (3) Starratt (2004), (4) Byrne et al. (2001), (5) Ingram et al. (1996), and (6) Ingram and DePaolo (1993).

discharge from the San Joaquin River. For example, evidence of an extreme flood event was found at ~ 530 cal yr BP (1420 CE) at Browns Island (Goman and Wells, 2000). During this period, BACHI had the lowest value of $\delta^{87}Sr$ for the entire record, which is also closest to the signature of the Sacramento River (Fig. 7d). Another possible explanation could be the migration of the confluence of the two rivers to points further east. Such a migration could have increased the relative proportion of Sacramento River water that flowed into the San Joaquin River as a result of tidal fluctuations.

Further west at FW, the salinity regime is slightly different than at BACHI. Throughout the entire record except in the two "modern" periods from ~1850 to ~1963 and ~1963 to present, the salinity regime has been fresh (Fig. 7c). During the periods ranging from 3600 BCE to 350 BCE, the San Joaquin River had especially strong influence at the site. This changed during the period from 350 BCE to 1450 CE when the Sacramento River gained importance. This pattern of increased importance of Sacramento River flows during this time period is found at all three sites (Fig. 7b–d). The Gold Rush period again proved to be distinctive during the two modern periods as the "apparent" salinity increased to over 4% (1.4 psu) (Fig. 7c).

Continuing west to BRI, there was clearly more variability in salinity at this western boundary of the Delta. The oldest samples, from 4350 to 1550 BCE, ranged between less than 1% up to ~2% psu, which encompasses the fresh to oligohaline range (Fig. 7b). Between 1550 and 350 BCE, BRI returned to being fresh and being dominated by Sacramento River water. During the period from 350 BCE to 1450 CE, the salinity regime was between 1.5% and 3% seawater, which is in the oligohaline range. The signal from the Gold Rush period was very strong, causing the apparent salinity to rise up to approximately 30%. Recent gauge data (Table 3) show BRI to be oligohaline, so, even excluding the anomalous isotopic record during the Gold Rush period, it is likely that BRI has been oligohaline for much of the recent record.

These conclusions for BRI are similar, but not identical to those of Goman and Wells (2000), who studied the paleosalinity of BRI using root/seed macrofossils as salinity proxies. Contrary to our findings, they concluded that there was a fresher period in the record between ~1850 BCE and 50 CE based on the presence of *Phragmites communis* (now called *Phragmites australis*; common reed) macrofossils. This emergent macrophyte is typically found in the fresher parts of the Delta, and, therefore, was thought to be indicative of periods of greater discharge from the rivers (Goman and Wells, 2000). However, *Phragmites australis* is a widely distributed plant in marshes, able to grow in both brackish and fresh waters (Mitsch and Gosselink, 1993, p. 609; Vasquez et al., 2005). Therefore, it is unclear whether this change in species distribution is indicative of fresh (or fresher on the oligohaline scale) conditions. Regardless, the data from this study as well as that of Goman and Wells (2000) clearly demonstrate that salinity at BRI (and likely other areas in the western Delta) has been perched at the ecotone between oligohaline and fresh for more than 6000 years.

6. Conclusions

The paleosalinity of the Sacramento-San Joaquin Delta of California, which is the landward most region of the San Francisco Estuary, was determined using a mixing model comprised of a combination of Sr and U concentrations and isotopic compositions of peat and the three main water sources. A proof of concept study demonstrated that $\delta^{87}Sr$ in the roots and rhizomes of the dominant marsh plant (*Schoenoplectus* spp.) varies with salinity in the Estuary. The values of the three water sources, the Sacramento River, San Joaquin River, and seawater, were distinct for $\delta^{87}Sr$, but the $^{234}U/^{238}U$ activity ratios of the San Joaquin River and seawater were almost indistinguishable. Nevertheless, when used in combination with $\delta^{87}Sr$ values, $^{234}U/^{238}U$ activity ratios were a highly effective tracer of the relative contributions of Sacramento and San Joaquin River water as long as seawater contributions remained low. These results indicate that the central Delta has been largely fresh (<0.5 ppt) for over the past 5000+ years, however rare spikes of salinity in the oligohaline range did occur during this time. The Sacramento vs. San Joaquin Rivers had varying degrees of hydrologic influence over the central Delta over the millennia, strongly suggesting shifts in flow volumes and/or the channel courses of these rivers. The western border of the Delta has been a transitional region perched at the ecotone between oligohaline and fresh for more than 6000 years. During the California Gold Rush period, a marked change in the $\delta^{87}Sr$ signature did not correlate with a recorded change in salinity, indicating that other causes, such as anthropogenic land use changes and hydraulic mining, were likely responsible for the anomalous $\delta^{87}Sr$ values.

Acknowledgments

We acknowledge the Delta Stewardship Council of the Resources Agency of California, which supported this research through contract # F-03-RE-029. We thank Peter Dileanis for providing data from the USGS NWIS database and Greg Brewster for collecting river water samples from the Sacramento and San Joaquin Rivers. We acknowledge Amber Powell for researching and drawing Fig. 8 and Yvonne Roque for creating the computer graphic. We thank Mike Torresan and Cathy Frassee for assisting with cold storage of peat cores during the project.

We appreciate the helpful and constructive comments of Christopher Fuller and two anonymous reviewers.

Appendix A. Supplementary material

Supplementary data associated with this article can be found, in the online version, at http://dx.doi.org/10.1016/j.apgeochem.2013.10.011.

References

Alpers, C.N., Hunerlach, M.P., 2000. Mercury contamination from historic gold mining in California. US Geol. Surv. Fact Sheet FS-061-00. <http://pubs.er.usgs.gov/publication/fs06100>.

Alpers, C.N., Drexler, J.Z., Neymark, L.A., Paces, J.B., Taylor, H.E., 2008. Minerogenic peat deposits of the Sacramento–San Joaquin Delta, California: a useful archive for anthropogenic contamination of mercury and lead. Report to the CALFED Science Program of the Resources Agency of California. <http://ca.water.usgs.gov/reports/repeat_pub_MercuryCALFED.pdf> (accessed 25.01.13).

Ames, L.L., McGarrah, J.E., Walker, B.A., 1983. Sorption of trace constituents from aqueous solutions onto secondary minerals. I. Uranium. Clays Clay Miner. 31, 321–334.

Andersson, P.S., Porcelli, D., Gustafsson, Ö., Ingri, J., Wasserburg, G.J., 2001. The importance of colloids for the behavior of uranium isotopes in the low-salinity zone of a stable estuary. Geochim. Cosmochim. Acta 65, 13–25.

Armentano, T.M., Woodwell, G.M., 1975. Sedimentation rates in a Long Island marsh determined by ^{210}Pb dating. Limnol. Oceanogr. 20, 452–456.

Atwater, B.F., 1980. Attempts to correlate late Quaternary climatic records between San Francisco Bay, the Sacramento-San Joaquin Delta, and the Mokelumne River, California. Ph.D. Dissertation. University of Delaware, Newark, DE, USA.

Barber, L.B., Keefe, S.H., Brown, G.K., Taylor, H.E., Antweiler, R.C., Peart, D.B., Plowman, T.I., Roth, D.A., Wass, R.D., 2003. Organic and trace element contaminants in water, biota, sediment, and semi-permeable membrane devices at Tres Rios Treatment Wetlands, Phoenix, AZ. US Geol. Surv. Wat. Res. Invest. Rep. 03-4129. <http://pubs.usgs.gov/wri/2003/4129/>.

Borovec, Z., 1981. The adsorption of uranyl species by fine clay. Chem. Geol. 32, 45–58.

Boss, C.B., Fredeen, K.J., 1999. Concepts, Instrumentation, and Techniques in Inductively Coupled Plasma Optical Emission Spectrometry. Perkin Elmer Corp., Norwalk, CT.

Bouse, R., Fuller, C.C., Luoma, S., Hornberger, M.I., Jaffe, B.E., Smith, R.E., 2010. Mercury-contaminated hydraulic mining debris in San Francisco Bay. San Francisco Estuary Water Sci. 8, 1–28.

Byrne, R., Ingram, B.L., Starratt, S., Malamud-Roam, F., Collins, J.N., Conrad, M.E., 2001. Carbon-isotope, diatom, and pollen evidence for late Holocene salinity change in a brackish marsh in the San Francisco Estuary. Quat. Res. 55, 66–76.

California Department of Water Resources, U.S. Bureau of Reclamation, U.S. Fish and Wildlife Service, and National Marine Fisheries Service. 2013. Environmental Impact Report/Environmental Impact Statement for the Bay Delta Conservation Plan. Administrative Draft. March. (ICF 00674.12.) Prepared by ICF International, Sacramento, CA. <http://baydeltaconservationplan.com/Libraries/Dynamic_Document_Library/EIR-EIS_Title_Page_and_Table_of_Contents_5-10-13.sflb.ashx> (accessed 18.09.13).

California Department of Water Resources, Division of Safety of Dams, 2009. Listing of Dams, California Data Exchange Center, State of California. <http://www.water.ca.gov/damsafety/damlisting/index.cfm>. (accessed 30.04.13).

Chabaux, F., Riotte, J., Dequincey, O., 2003. U–Th–Ra fractionation during weathering and river transport. In: Bourdon, B., Henderson, G.M., Lundstrom, C.C., Turner, S.P. (Eds.), Uranium-Series Geochemistry. Reviews of Mineralogy and Geochemistry, vol. 52, pp. 533–576.

Chabaux, F., Bourdon, B., Riotte, J., 2008. U-series geochemistry in weathering profiles, river waters and lakes. In: Krishnaswami, S., Cochran, J.K. (Eds.), U/Th Series Radionuclides in Aquatic Systems. Radioactivity in the Environment, vol. 13, pp. 49–104.

Charman, D., 2002. Peatlands and Environmental Change. John Wiley and Sons Ltd., Chichester.

Cheng, H., Edwards, R.L., Hoff, J., Gallup, C.D., Richards, D.A., Asmerom, Y., 2000. The half-lives of uranium-234 and throium-230. Chem. Geol. 169, 17–33.

Cowardin, L.M., Carter, V., Golet, F.C., LaRoe, E.T., 1979. Classification of Wetlands and Deepwater Habitats of the United States. FWS/OBS-79/31, US Fish and Wildlife Service, Washington, DC.

Delanghe, D., Bard, D., Hamelin, B., 2002. New TIMS constraints on the uranium-238 and uranium-234 in seawaters from the main ocean basins and Mediterranean Sea. Mar. Chem. 80, 79–93.

DeLaune, R.D., Baumann, R.H., Gosselink, J.G., 1983. Relationships among vertical accretion, coastal submergence, and erosion in a Louisiana Gulf coast marsh. J. Sediment. Petrol. 53, 147–157.

Di Rita, F., Simone, O., Caldara, M., Gehrels, W.R., Magri, D., 2011. Holocene environmental changes in the coastal Tavoliere Plain (Apulia, southern Italy): a multiproxy approach. Palaeogeogr. Palaeoclimatol. Palaeoecol. 310, 139–151.

Domagalski, J., 2001. Mercury and methylmercury in water and sediment of the Sacramento River Basin, California. Appl. Geochem. 16, 1677–1691.

Drexler, J.Z., 2011. Peat formation processes through the millennia in tidal marshes of the Sacramento–San Joaquin Delta, California, USA. Estuaries Coast. <http://dx.doi.org/10.1007/s12237-011-9393-7>.

Drexler, J.Z., de Fontaine, C.S., Knifong, D.L., 2007. Age determination of the remaining peat in the Sacramento-San Joaquin Delta, California, USA. US Geol. Surv. Open-File Rep. 2007-1303. <http://pubs.er.usgs.gov/publication/ofr20071303>.

Drexler, J.Z., de Fontaine, C.S., Brown, T.A., 2009a. Peat accretion histories during the past 6000 years in marshes of the Sacramento–San Joaquin Delta, CA, USA. Estuaries Coast 32, 871–892.

Drexler, J.Z., de Fontaine, C.S., Deverel, S.J., 2009b. The legacy of wetland drainage on peat resources in the Sacramento – San Joaquin Delta, California, USA. Wetlands 29, 372–386.

Dunk, R.M., Mills, R.A., Jenkins, W.J., 2002. A reevaluation of the oceanic uranium budget for the Holocene. Chem. Geol. 190, 45–67.

Faure, G., 1986. Principles of Isotope Geology, second ed. John Wiley & Sons, New York.

Faure, G., Mensing, T.M., 2005. Isotopes – Principles and Applications, third ed. John Wiley & Sons, New York.

Faure, G., Powell, J.L., 1972. Strontium Isotope Geology. Springer-Verlag, New York.

Florsheim, J.L., Mount, J.F., 2003. Changes in lowland floodplain sedimentation processes: pre-disturbance to post-rehabilitation, Cosumnes River, CA. Geomorphology 56, 305–323.

Foster, I.D.L., Mighall, T.M., Proffitt, H., Walling, D.E., Owens, P.N., 2006. Post-depositional ^{137}Cs mobility in the sediments of three shallow coastal lagoons, SW England. J. Paleolimnol. 35, 881–895.

Gambrell, R.P., Patrick Jr., W.H., 1978. Chemical and microbiological properties of anaerobic soils and sediments. In: Hook, D.D., Crawford, R.M.M. (Eds.), Plant Life in Anaerobic Environments. Ann Arbor Science Publishers Inc., pp. 375–423.

Ganju, N.K., Schoellhamer, D.H., Bergamaschi, B.A., 2005. Suspended sediment fluxes in a tidal wetland: measurement, controlling factors, and error analysis. Estuaries 28, 812–822.

Garbarino, J.R., Taylor, H.E., 1979. An inductively coupled plasma-atomic emission spectrometric technique for water quality testing. Appl. Spectrosc. 33, 220–226.

Garbarino J.R., Taylor, H.E., 1996. Inductively coupled plasma-mass spectrometric method for the determination of dissolved trace elements in natural water: US Geol. Surv. Open-File Rep. No. 94-358, 88p.

Gascoyne, M., 1992. Geochemistry of the actinides and their daughters. In: Ivanovich, M., Harmon, R.S. (Eds.), Uranium-Series Disequilibrium: Applications to Earth, Marine, and Environmental Sciences, second ed. Clarendon Press, Oxford, pp. 34–61.

Gilbert, G.K., 1917. Hydraulic-mining Debris in the Sierra Nevada. US Geological Survey professional paper 105. US Government Printing Office, Washington, DC.

Givelet, N., Le Roux, G., Cheburkin, A., Chen, B., Frank, J., Goodsite, M., Kempter, H., Krachler, M., Noernberg, T., Rausch, N., Rheinberger, S., Roos-Barraclough, F., Sapkota, A., Scholz, C., Shotyk, W., 2004. Suggested protocol for collecting, handling and preparing peat cores and peat samples for physical, chemical, mineralogical and isotopic analyses. J. Environ. Monitor. 6, 481–492.

Goman, M., 2001. Statistical analysis of modern seed assemblages from the San Francisco Bay: applications for the reconstruction of paleo-salinity and paleo-tidal inundation. J. Paleolimnol. 24, 393–409.

Goman, M., Wells, L., 2000. Trends in river flow affecting the northeastern reach of the San Francisco Bay Estuary over the past 7000 years. Quat. Res. 54, 206–217.

Hart, W.S., Quade, J., Madsen, D.B., Kaufmann, D.S., Ovitt, C.G., 2004. The ^{87}Sr/^{86}Sr ratios of lacustrine carbonates and lake-level history of the Bonneville paleolake system. Geol. Soc. Am. Bull. 116, 1107–1119.

Hart, R.J., Taylor, H.E., Antweiler R.C., Graham, D.D., Fisk, G.G., Riggins, S.G., Flynn, M.E., 2005. Sediment chemistry of the Colorado River delta of Lake Powell, UT, 2001. US Geol. Surv. Open-File Rep. 2005-1178. <http://pubs.er.usgs.gov/publication/ofr20051178>.

Heegaard, E., Birks, H.J.B., Telford, R.J., 2005. Relationships between calibrated ages and depth in stratigraphical sequences: an estimation procedure by mixed-effect regression. Holocene 15, 612–618.

Heiri, O., Lotter, A.F., Lemcke, G., 2001. Loss on ignition as a method for estimating organic and carbonate content in sediments; reproducibility and comparability of results. J. Paleolimnol. 25, 101–110.

Hobbs, J.A., Lewis, L.S., Ikemiyagi, N., Sommer, T., Baxter, R.D., 2010. The use of otolith strontium isotopes (^{87}Sr/^{86}) to identify nursery habitat for a threatened estuarine fish. Environ. Biol. Fish. <http://dx.doi.org/10.1007/s10641-010-9672-3>.

Hodell, D.A., Mead, G.A., Mueller, P.A., 1990. Variation in the strontium isotopic composition of seawater (8 Ma to present): implications for chemical weathering rates and dissolved fluxes to the oceans. Chem. Geol. 80, 291–307.

Hornberger, M.I., Luoma, S.N., van Geen, A., Fuller, C.C., Anima, R., 1999. Historical trends of metals in the sediments of San Francisco Bay, California. Mar. Chem. 64, 39–55.

Idiz, E.F., Carlisle, D., Kaplan, I.R., 1986. Interaction between organic matter and trace metals in a uranium rich bog, Kern County, California, USA. Appl. Geochem. 1, 573–590.

Ingebritsen, S.E., Ikehara, M.E., Gallaway, D.L., Jones, D.R., 2000. Delta subsidence in California: the sinking heart of the state. US Geol. Surv. Fact Sheet FS-005-00. <http://pubs.er.usgs.gov/publication/fs00500>.

Ingram, B.L., DePaolo, D.J., 1993. A 4300 strontium isotope record of estuarine paleosalinity in San Francisco Bay, California. Earth Planet. Sci. Lett. 119, 103–119.

Ingram, B.L., Sloan, D., 1992. Strontium isotopic composition of estuarine sediments as paleosalinity/paleoclimate indicator. Science 255, 68–72.

Ingram, B.L., Ingle, J.C., Conrad, M.E., 1996. A 2000 yr record of Sacramento-San Joaquin river inflow to San Francisco Bay estuary, California. Geology 24, 331–334.

Jaffey, A.H., Flynn, K.F., Glendenin, L.E., Bentley, W.C., Essling, A.M., 1971. Precision measurements of half-lives and specific activities of ^{235}U and ^{238}U. Phys. Rev. C 4, 1889–1906.

Johnson, S.Y., Otton, J.K., Macke, D.I., 1987. Geology of the Holocene surficial uranium deposit in north fork of Flodelle Creek, northeastern Washington. Geol. Soc. Am. Bull. 98, 77–85.

Kigoshi, K., 1971. Alpha-recoil thorium-234: dissolution into water and the uranium-234/uranium-238 disequilibrium in nature. Science 173, 47–48.

Kimmerer, W.J., 2002. Physical, biological, and management responses to variable freshwater flow into the San Francisco Estuary. Estuaries 25, 1275–1290.

López-Buendia, A.M., Bastida, J., Querol, X., Whateley, M.K.G., 1999. Geochemical data as indicators of palaeosalinity in coastal organic-rich sediments. Chem. Geol. 157, 235–254.

Ludwig, K.R., Wallace, A.R., Simmons, K.R., 1985. The Schwartzwalder uranium deposit, II: age of uranium mineralization and Pb-isotope constraints on genesis. Econ. Geol. 80, 1858–1871.

MacKenzie, A.B., Farmer, J.G., Sugden, C.L., 1997. Isotopic evidence of the relative retention and mobility of lead and radiocaesium in Scottish ombrotrophic peats. Sci. Total Environ. 203, 115–127.

Malamud-Roam, F., Ingram, B.L., 2004. Late Holocene ^{13}C and pollen records of paleosalinity from tidal marshes in the San Francisco Bay estuary, California. Quat. Res. 64, 134–145.

May, M.D., 1999. Vegetation and salinity changes over the last 2,000 years at two islands in the northern San Francisco Estuary, California. Master's thesis. University of California, Berkeley, CA, USA.

McArthur, J.M., Howarth, R.J., Bailey, R.R., 2001. Strontium isotope stratigraphy: LOWESS version 3: best fit to the marine Sr-isotope curve for 0–509 Ma and accompanying look-up table for deriving numerical age. J. Geol. 109, 155–170.

McArthur, J.M., Rio, D., Massari, F., Castradori, D., Bailey, T.R., Thirlwall, M., Houghton, S., 2006. A revised Pliocene record for marine-^{87}Sr/^{86}Sr used to date an interglacial event recorded in the Cockburn Island Formation, Antarctic Peninsula. Palaeogeogr. Palaeoclimatol. Palaeoecol. 242, 126–136.

McKee, B.A., 2008. U-Th series nuclides in aquatic systems. In: Krishnaswami, S., Cochran, J.K. (Eds.), Radioactivity in the Environment, vol. 13. Elsevier Ltd., Amsterdam, pp. 193–225.

Mitsch, W.J., Gosselink, J.G., 1993. Wetlands. Van Nostrand Reinhold, New York.

Neymark, L.A., Amelin, Y.V., 2008. Natural radionuclide mobility and its influence on U–Th–Pb dating of secondary minerals from the unsaturated zone at Yucca Mountain, Nevada. Geochim. Cosmochim. Acta 72, 2067–2089.

Novak, M., Zemanova, L., Voldrichova, P., Stepanova, M., Adamova, M., Pacherova, P., Komarek, A., Krachler, M., Prechova, E., 2011. Experimental evidence for mobility/immobility of metals in peat. Environ. Sci. Technol. 45, 7180–7187.

Owen, D.E., Otton, J.K., Hills, F.A., Schumann, R.R., 1992. Uranium and other elements in Colorado Rocky Mountain wetlands – a reconnaissance study, US Geol. Surv. Bull., 1992, US Government Printing Office, Denver.

Peros, M.C., Reinhardt, E.G., Schwarcz, H.P., Davis, A.M., 2007. High-resolution paleosalinity reconstruction from Laguna de la Leche, north coastal Cuba, using Sr, O, and C isotopes. Palaeogeogr. Palaeoclimatol. Palaeoecol. 245, 535–550.

Peterson, D.H., Cayan, R.C., Festa, J.F., Nichols, F.H., Walters, R.A., Slack, J.V., Hager, S.E., Schemel, L.E., 1989. Climate variability in an estuary: effects of riverflow on San Francisco Bay. In: Peterson, D.H. (Ed.), Aspects of Climate Variability in the Pacific and Western Americas. American Geophysical Union Geophysical Monographs, vol. 55, Washington, DC, pp. 419–442.

Porcelli, D., 2008. Investigating groundwater processes using U- and Th-series nuclides. In: Krishnaswami, S., Cochran, J.K. (Eds.), U/Th Series Radionuclides in Aquatic Systems. Radioactivity in the Environment, vol. 13. Elsevier, Oxford, pp. 105–153.

Prokopovich, N.P., 1985. Subsidence of peat in California and Florida. Bull. Assoc. Eng. Geol. 22, 395–420.

Prokopovich, N.P., 1988. Tectonic subsidence in California's Sacramento-San Joaquin "Delta". Bull. Assoc. Eng. Geol. 25, 140–144.

Rabenhorst, M.C., 2001. Soils of tidal and fringing wetlands. In: Richardson, J.L., Vepraskas, M.J. (Eds.), Wetland Soils: Genesis, Hydrology, Landscapes, and Classification. CRC Press LCC, pp. 301–315.

Reimer, P.J., Baillie, M.G.L., Bard, E., Bayliss, A., Beck, J.W., Bertrand, C.J.H., Blackwell, P.G., Buck, C.E., Burr, G.S., Cutler, K.B., Damon, P.E., Edwards, R.L., Fairbanks, R.G., Friedrich, M., Guilderson, T.P., Hogg, A.G., Hughen, K.A., Kormer, B., McCormac, G., Manning, S., Ramsey, C.B., Reimer, R.W., Remmele, S., Southon, J.R., Stuiver, M., Talamo, S., Taylor, F.W., van der Plicht, J., Weyhenmeyer, C.E., 2004. IntCal04 terrestrial radiocarbon age calibration, 0–26 cal kyr BP. Radiocarbon 46, 1029–1058.

Ritchie, J.C., McHenry, J.R., 1990. Application of radioactive fallout cesium-137 for measuring soil erosion and sediment accumulation rates and patterns: a review. J. Environ. Qual. 19, 215–233.

Rojstaczer, S.A., Hamon, R.E., Deverel, S.J., Massey, C.A., 1991. Evaluation of Selected Data to Assess the Causes of Subsidence in the Sacramento-San Joaquin Delta, California. US Geol. Surv. Open-File Rep. 91-0193. <http://pubs.er.usgs.gov/publication/91193>.

Roth, D.A., Antweiler, R.C., Brinton, T.I., Taylor, H.E., 1997. Major and trace elements, Chapter 5. In: Moody, J.A. (Ed.), Hydrologic, Sedimentologic, and Chemical Data Describing Surficial Bed Sediments in Navigational Pools in the Upper Mississippi River, After the Flood of 1993. US Geol. Surv. Open-File Rep. 96-580. <http://pubs.er.usgs.gov/publication/ofr96580>.

Shand, P., Darbyshire, D.P.F., Gooddy, D., Haria, A.H., 2007. $^{87}Sr/^{86}$ as an indicator of flowpaths and weathering rates in the Plynlimon experimental catchments, Wales, UK. Chem. Geol. 236, 247–265.

Shlemon, R.J., Begg, E.L., 1975. Late Quaternary evolution of the Sacramento-San Joaquin delta, California. In: Suggate, R.P., Cressel, M.M. (Eds.), Quaternary Studies. Bulletin, vol. 13. The Royal Society of New Zealand, Wellington, pp. 59–266.

Shotyk, W., 1996. Peat bog archives of atmospheric metal deposition: geochemical assessment of peat profiles, natural variations in metal concentrations, and metal enrichment factors. Environ. Rev. 4, 149–183.

Stahle, D.W., Therrell, M.D., Cleaveland, M.K., 2001. Ancient blue oaks reveal human impact on San Francisco Bay salinity. Eos 82, 12. <http://dx.doi.org/10.1029/EO082i012p00141>.

Starratt, S.W., 2004. Diatoms as indicators of late Holocene freshwater flow variation in the San Francisco Bay estuary, central California, USA. In: Poulin, M. (Ed.), Proceedings of the Seventeenth International Diatom Symposium 2002. Biopress, Devon, pp. 71–397.

Steiger, R.H., Jäger, E., 1977. Subcommission on geochronology: convention on the use of decay constants in geo- and cosmochronology. Earth Planet. Sci. Lett. 36, 359–362.

Stuiver, M., Reimer, P.J., 1993. Extended ^{14}C data base and revised CALIB 3.0 14C age calibration program. Radiocarbon 35, 215–230.

Swarzenski, P.W., Porcelli, D., Andersson, P.S., Smoak, J.M., 2003. The behaviour of U- and Th-series nuclides in the estuarine environment. In: Bourdon, B., Henderson, G.M., Lundstrom, C.C., Turner, S.P. (Eds.), Uranium-series geochemistry. Reviews of Mineralogy and Geochemistry, vol. 52, pp. 577–606.

Szalay, A., 1964. Cation exchange properties of humic acids and their importance in the geochemical enrichment of UO_2^{+2} and other cations. Geochim. Cosmochim. Acta 28, 1605–1614.

Taylor, H.E., 2001. Inductively Coupled Plasma-mass spectrometry: Practices and Techniques. Academic Press, San Diego.

The Bay Institute, 2003. The 2003 San Francisco Bay Index. Novato, CA. <http://www.bay.org/assets/Executive_Summary.pdf> (accessed 23.09.12).

Thompson, J., 1957. The settlement geography of the Sacramento-San Joaquin Delta, California. Ph.D. Dissertation. Stanford University, Stanford, CA.

Turekian, K.K., 1968. Oceans, second ed. Prentice-Hall, New Jersey.

Turetsky, M.R., Manning, S.W., Wieder, R.K., 2004. Dating recent peat deposits. Wetlands 24, 324–356.

Van der Putten, N., Mauquoy, D., Verbruggen, C., Björck, S., 2012. Subantarctic peatlands and their potential as palaeoenvironmental and palaeoclimatic archives. Quat. Int. 268, 65–76.

Van Metre, P.C., Fuller, C.C., 2009. Dual-core mass-balance approach for evaluating mercury and lead atmospheric fallout and focusing to lakes. Environ. Sci. Technol. 43, 26–32.

Vasquez, E.A., Glenn, E.P., Brown, J.J., Guntenspergen, G.R., Nelson, S.G., 2005. Salt tolerance underlies the cryptic invasion of North American salt marshes by an introduced haplotype of the common reed *Phragmites australis* (Poaceae). Mar. Ecol. Prog. Ser. 298, 1–8.

von Carnap-Bornheim, C., Nosch, M.-L., Grupe, G., Mekota, A.-M., Schweissing, M.M., 2007. Stable strontium isotopic ratios from archaeological organic remains from the Thorsberg peat bog. Rapid Commun. Mass Spectrom. 21, 1541–1545.

Weir, W.W., 1950. Subsidence of peat land of the Sacramento-San Joaquin Delta, California. Hilgardia 20, 37–56.

Westcot, D.W., Chilcott, J.E., Wright, T.S., 1992. Water Quality of the Lower San Joaquin River: Lander Avenue to Vernalis, October 1990 to September 1991 (Water Year 1991). Staff Report of the California Regional Water Quality Control Board Central Valley Region. <http://www.swrcb.ca.gov/rwqcb5//water_issues/swamp/historic_reports_and_faq_sheets/sjr_wq/92_sjr_wtrqty_90_91.pdf> (accessed 30.09.12).

Wright Jr., H.E., 1991. Coring tips. J. Paleolimnol. 6, 37–49.

Zielinski, R.A., Simmons, K.R., Orem, W.H., 2000. Use of ^{234}U and ^{238}U isotopes to identify fertilizer-derived uranium in the Florida Everglades. Appl. Geochem. 15, 369–383.